Journal of Molecular Liquids 337 (2021) 116396

Contents lists available at ScienceDirect

Journal of Molecular Liquids

journal homepage: www.elsevier.com/locate/molliq

CO_2-binding organic liquids for high pressure CO_2 absorption: Statistical mixture design approach and thermodynamic modeling of CO_2 solubility using LJ-Global TPT2 EoS

Ali Hedayati, Farzaneh Feyzi *

Thermodynamics Research Laboratory, School of Chemical Engineering, Iran University of Science and Technology, Tehran 1684613114, Iran

ARTICLE INFO

Article history:
Received 13 January 2021
Revised 27 April 2021
Accepted 2 May 2021
Available online 11 May 2021

Keywords:
Switchable ionic liquids
Thermodynamic modeling
CO_2 solubility
Mixture design
LJ-Global TPT2 EoS

ABSTRACT

CO_2-binding organic liquids (CO_2-BOLs) or switchable ionic liquids (SILs) are switchable polarity solvents (SPS) that can be used as non-aqueous, energy efficient solvents for CO_2 absorption. In this study, the three-component CO_2-BOLs comprised of a single-component CO_2-BOL (tertiary alkanolamine) and a two-component CO_2-BOL (superbase/alcohol) are introduced. The most efficient equimolar combination of superbase (1,8-diazabicyclo-[5.4.0]-undec-7-ene (DBU)), alcohol (methanol, n-butanol, *sec*-butanol, *tert*-butanol and hexanol) and amine (Dimethylethanolamine (DMEA), Diethylethanolamine (DEEA) and N-methyldiethanolamine (MDEA)) are obtained using screening experiments considering CO_2 loading (α_{eq}) and absorption rate (α_R). The mixture design technique is employed for modeling of α_{eq} and α_R as a function of mole fraction of components at 35.0 °C and initial pressure of 25.0 bar. The DBU/DMEA/n-butanol CO_2-BOL represented the best performance for CO_2 uptake. The experimental CO_2 solubility data in DBU/n-butanol, DBU/DMEA and DBU/DMEA/n-butanol BOLs were obtained in the temperature range of 25.0–45.0 °C and the pressure range of 1.0–45.0 bar. The DBU mole fraction was selected to be 0.1 and 0.2 while the molar ratio of DMEA to n-butanol was kept constant at 2 in the three-component BOL. The simultaneous vapor–liquid and chemical equilibrium calculation algorithm using LJ-Global TPT2 equation of state was used for the thermodynamic modeling of CO_2 solubility in BOLs. The average absolute relative deviation error (AAD%) for the calculation of total pressure of DBU/n-butanol, DBU/DMEA and DBU/DMEA/n-butanol BOLs were obtained to be 8.5%, 5.8% and 8.6%, respectively.

1. Introduction

Global warming has become a serious environmental issue due to CO_2 emission into the atmosphere as a greenhouse gas (GHG) [1]. CO_2 is produced mainly from several anthropogenic activities like combustion of fossil fuels and carbonates decomposition [2]. To reduce the CO_2 concentration in atmosphere, CO_2 capture technologies are designed [3,4]. CO_2 removal from natural gas is also an important processing step to produce high quality gas streams [5].

Chemical CO_2 trapping agents like aqueous amine solutions rapidly bind CO_2 to produce water-soluble carbamate and bicarbonate salts, effective for post-combustion capture where the CO_2 concentration is very low (5–15 vol%) [6]. However, this approach suffers from considerable drawbacks including: high energy consumption for solvent regeneration, low capture efficiency and kinetics, corrosive nature and volatility of amines. The ethanolamine concentration rarely exceeds 30 wt% because of the corrosive nature of solvent which reduces the maximum CO_2 absorption ($\leq$108 g L^{-1} or $\leq$ 7 wt%). The low concentration of ethanolamine leads to pumping and heating of large excess of water during CO_2 absorption and release which increases the energy consumption. These deficiencies have led to the development of other solvent systems [7].

A switchable solvent is defined as a solvent that reversibly converts its physicochemical properties upon contact with a trigger [8]. Switchable polarity solvents (SPSs) are a subclass of switchable solvents that switch from a lower polarity to a higher polarity form [9]. Switchable ionic liquids (SILs) or CO_2-binding organic liquids (CO_2-BOLs) are CO_2-triggered SPSs that readily switch from a non-ionic liquid mixture to an ionic liquid [10]. Unlike traditional ionic liquids, SILs are non-ionic before the reaction of solvent with CO_2 as the stimulus. Traditional ILs functionalized with terminal amines have moderate absorption capacity, such that, the amine tethered Immidazolium IL absorbs 0.5 M equivalents of CO_2 (7.4%

* Corresponding author.
E-mail addresses: ali_hedayati@chemeng.iust.ac.ir (A. Hedayati), feyzi@iust.ac.ir (F. Feyzi).

https://doi.org/10.1016/j.molliq.2021.116396
0167-7322/

CO_2 by weight) as carbamate salt within three hours to reach equilibrium condition [11]. Moreover, CO_2-BOLs do not contain CO_2 trapping functional groups and therefore have the potential for higher weight capacities of CO_2.

CO_2-BOLs are potential solvents for CO_2 capture due to their high selectivity towards CO_2 under a N_2 atmosphere, absorption efficiency, regeneration efficiency, recyclability and easy synthesis protocols. CO_2-BOLs reversibly bind CO_2 with a high gravimetric and volumetric capacity. There is no need for superfluous inert solvents in CO_2-BOLs due to their liquid nature before and after reacting with CO_2 that increases the absorption capacity [12].

The DBU/1-hexanol CO_2-BOL captures 1.3 mol of CO_2/mol DBU (19 wt% or 147 g CO_2 L^{-1} liquid), the additional 0.3 (4 wt%) is because of physical rather than chemical absorption. The combination of chemical and physical absorption results in higher CO_2 gravimetric capacity and volumetric capacity than aqueous ethanolamine systems (7 wt%, 108 g L^{-1} liquid) for 30% MEA in water [13]. In comparison with currently employed aqueous alkanolamine systems, CO_2-BOLs are much more energy efficient for CO_2 release. CO_2 bound more weakly in an alkylcarbonate salt (product of CO_2 reaction with CO_2-BOLs) rather than bicarbonate or carbamate salts (products of aqueous amine scrubbing systems) due to the decreased hydrogen bonding. Therefore, less energy is required to thermally strip the CO_2 from the liquid such that CO_2 release from some CO_2-BOLs occur at temperatures as low as room temperature [14]. The high specific heat of water (4.18 J g^{-1} deg^{-1} vs 1.2–2.0 J g^{-1} deg^{-1} for SILs) and solvent loss due to the heating of liquid above the boiling point of the solvent leads to the large inefficiency of MEA systems [15].

The most studied two-component CO_2-BOLs consist of a superbase (amidine or guanidine) and an alcohol or amino alcohol producing amidinium or guanidinium alkylcarbonate salts in the presence of CO_2 [15]. Also, two-component BOLs comprised of amidines/amino-acid esters [16], amidines/chiral amino alcohols [17] and amidines/aliphatic primary amines [18] to produce amidinium carbamates have been investigated. Single-component BOLs were also introduced for CO_2 absorption [19] as simpler systems which maintain clean CO_2 stream upon IL reversal due to no precursor evaporation [20].

In addition to single and two-component BOLs, mixtures of two-component BOLs and promoters were also studied for CO_2 capture. The mixture of 1,8-diazabicyclo-[5.4.0]-undec-7-ene (DBU)/ethanol SIL and aminomethyl propanol (AMP) was examined for CO_2 absorption by Liu et al. [21]. The absorption loading of DBU/AMP/ethanol at the optimum composition of 50 wt% ethanol and equimolar DBU and AMP was determined to be 2.98 mol/kg solvent. The produced solvent decreased the loading and absorption rate, while reduced the viscosity and enhanced the efficiency of solvent regeneration compared to the DBU/ethanol SIL. Orhan and Alper [22] studied the reaction kinetics of CO_2 absorption by SILs (hexanol/DBU and hexanol/1,1,3,3-tetramethylguanidine (TMG)) promoted by piperazine (PZ) (0–0.25 kmol/m^3) and its derivatives at 298 K while the base concentration was kept constant at 10 wt%. The relatively low reaction rates of the SILs were notably increased by the superbase/hexanol/PZ blend. However, alkyl carbamate salt is produced as a result of CO_2 reaction with the promoted two-component BOLs in the above mentioned studies. Recently, the amine promoted two-component BOLs based on DBU (DBU/alcohol/amine) and TMG (TMG/Alcohol/amine) were introduced by Hedayati and Feyzi [23,24] for CO_2 capture. It was observed that the addition of monoethanolamine (MEA) as a promoter to the two-component BOLs inhibits the formation and precipitation of bicarbonate salt in the presence of water that results in the lower energy consumption in the solvent regeneration step. Moreover, the equilibrium CO_2 loading was higher in the amine-promoted system compared to two-component BOLs.

Tertiary alkanolamines are pressure-sensitive solvents that chemically react with CO_2 to produce zwitterionic alkylammonium alkylcarbonate liquids and decarboxylate upon depressurization such that they act like physical sorbents. Rainbolt et al. [25] showed that anhydrous Dimethylethanolamine (DMEA) behaves as a hybrid (physical and chemical) CO_2 sorbent with up to 20 wt % CO_2 loading at 20.7 bar. CO_2 absorption rate and equilibrium uptake can be improved by addition of an alcohol and a superbase, respectively. Moreover, easier solvent regeneration can be achieved by addition of a tertiary alkanolamine to the two-component BOLs (superbase/alcohol). Single-component CO_2-BOLs (tertiary alkanol amines) combined with two-component CO_2-BOLs (base/alcohol) and produce alkyl carbonate salts upon reaction with CO_2 (Fig. 1). The unique property of the proposed BOLs is no carbamate species production in the solvent mixture after the reaction with CO_2 which facilitates its reversibility to the non-ionic form and reduces the required solvent regeneration energy.

In this study, for the first time, the three-component CO_2-BOLs (or SILs) comprised of a superbase (DBU), an alcohol (methanol, n-butanol, *sec*-butanol, *tert*-butanol and hexanol) and a tertiary alkanolamine, DMEA, Diethylethanolamine (DEEA) and N-methyldiethanolamine (MDEA)) are used as solvents for CO_2 absorption. CO_2 loading and absorption rate are obtained and evaluated.

Screening experiments and mixture design technique were implemented to investigate the effect of component type and proportion on the CO_2 loading and absorption rate. The experimental CO_2 solubility data were measured for the selected two-component and three-component BOLs. The phase equilibrium data were used for thermodynamic modeling of CO_2 solubility in the BOLs. The φ-φ approach by LJ-Global TPT2 equation of state (EoS) [26–28] was implemented to model the CO_2 solubility in the BOLs.

2. Experimental

2.1. Chemicals

Methanol (purity ≥ 99.9%), n-butanol (purity ≥ 99.5%), *sec*-butanol (purity ≥ 99.0%), *tert*-butanol (purity ≥ 99.5%), 1-hexanol (purity ≥ 98.0%), DBU (purity ≥ 98.0%) and amines were all purchased from Merck. All chemicals were distilled and dried to bring the water concentration to<20 ppm. High purity CO_2 from Roham Gas Co. (purity > 99.9%) was used in absorption experiments. Table 1 shows the name, acronym and chemical structure of the base and amines used in this study.

2.2. CO_2 absorption: Apparatus and procedure

The schematic of CO_2 absorption equipment is presented in Fig. 2. The employed method for gathering equilibrium solubility loading (α_{eq}) and absorption rate (α_R) data is available in the previous publications [23,24]. α_{eq} is defined as the number of absorbed CO_2 molecules per number of moles of solvent at equilibrium, while, as a measure of CO_2 absorption rate, α_R is the number of absorbed CO_2 molecules within 20 min per number of moles of solvent. The set-up and procedures were also validated by comparing the CO_2 solubility data in 15 and 30 mass percent aqueous MEA solutions in our previous work [24] with the results of Wagner et al. [29].

CO_2 loading (α) was calculated as follows:

$$\alpha = \frac{n^{l}_{CO_2}}{n_{solvent}} \quad (1)$$

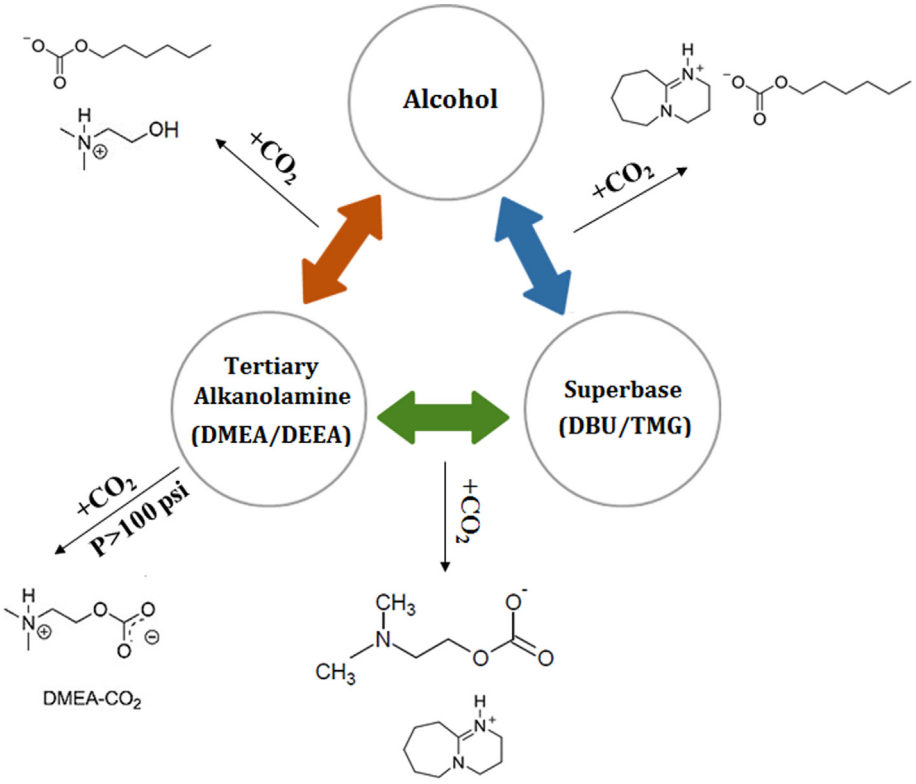

Fig. 1. The three-component switchable ionic liquid comprised of a superbase, an alcohol and a tertiary alkanol amine.

Table 1
Name, acronym and chemical structure of the base and amines in this study.

Name	Acronym	Molecular structure	purity
1,8-Diazabicyclo(5.4.0)undec-7-ene	DBU	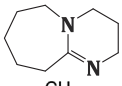	≥ 98.0%
Dimethyl ethanolamine	DMEA	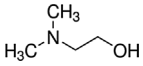	≥ 99.0%
Diethyl ethanolamine	DEEA	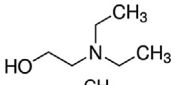	≥ 99.0%
Methyl diethanolamine	MDEA	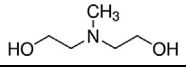	≥ 98.0%

where $n_{solvent}$ and $n^{l}_{CO_2}$ are defined as the total number of moles of solvent and the number of moles of absorbed CO_2 into the solvent (Eq. (2)):

$$n^{l}_{CO_2} = n_{CO_2} - n^{g}_{CO_2} \tag{2}$$

In Eq. (2) n_{CO_2} and $n^{g}_{CO_2}$ are the number of moles of injected CO_2 into the autoclave from the gas container and the number of moles of unabsorbed CO_2 in the gas phase which were calculated from Eqs. (3) and (4), respectively.

$$n_{CO_2} = \frac{V_{gc}}{R}\left(\frac{P_1}{Z_1 T_1} - \frac{P_2}{Z_2 T_2}\right) \tag{3}$$

$$n^{g}_{CO_2} = \frac{V_g P_{CO_2}}{Z_{CO_2} RT} \tag{4}$$

$$P_{CO_2} = P_t - P^{*}_{s} \tag{5}$$

$$V_g = V - V_s \tag{6}$$

Z, R,P_{CO_2}, V_g, , V_{gc}, P, T, P_t , P^{*}_{s}, V and V_s are the compressibility factor (calculated by the Peng-Robinson EOS [30]), the universal gas constant, equilibrium pressure of CO_2, gas phase volume in the autoclave, volume of gas container, pressure and temperature of gas container, the total pressure of the autoclave reactor, the vapor pressure of the solvent, the volume of the autoclave and volume of the injected solvent, respectively.

The uncertainty of the calculated CO_2 loading values was evaluated by the error propagation method by Eq. (7) [31].

$$\delta f = \pm\sqrt{\left(\frac{\partial f}{\partial x}\partial x\right)^2 + \cdots + \left(\frac{\partial f}{\partial z}\partial z\right)^2} \tag{7}$$

where $(x, \ldots, z)$, $f\,(x, \ldots, z)$ and $(dx, \ldots, dz)$ are the measured quantities, the calculated variable and uncertainties. The uncertainty in determination of α_{eq} was assessed by considering the errors in measuring quantities including: temperature, pressure, volume of the gas containers and autoclave, mass of solvent (m) and the compressibility factor calculated from the Peng-Robinson EoS. The uncertainties of the variables are: $P_{total} = \pm 2.5\text{KPa}$, $\delta P^{sat}_{solution} = \pm 2.5\text{KPa}$, $\delta T = \pm 0.1\text{K}$, $\delta V = \pm 10^{-6}\text{m}^3$, $\delta m = \pm 10^{-7}\text{Kg}$. Also, the uncertainty of CO_2 equilibrium pressure and compressibility factor were calculated to be $\delta P_{CO_2} = \pm 3.53\text{KPa}$ and $\delta Z = \pm 0.0092$, repectively. The obtained uncertainties for equilibrium CO_2 solubility is discussed in Section 4.3.3.

3. Thermodynamic framework

The CO_2 uptake into BOLs is explained by simultaneous phase and chemical reaction equilibrium. The φ-φ approach using LJ-Global TPT2 EoS [26–28] is implemented for modeling CO_2

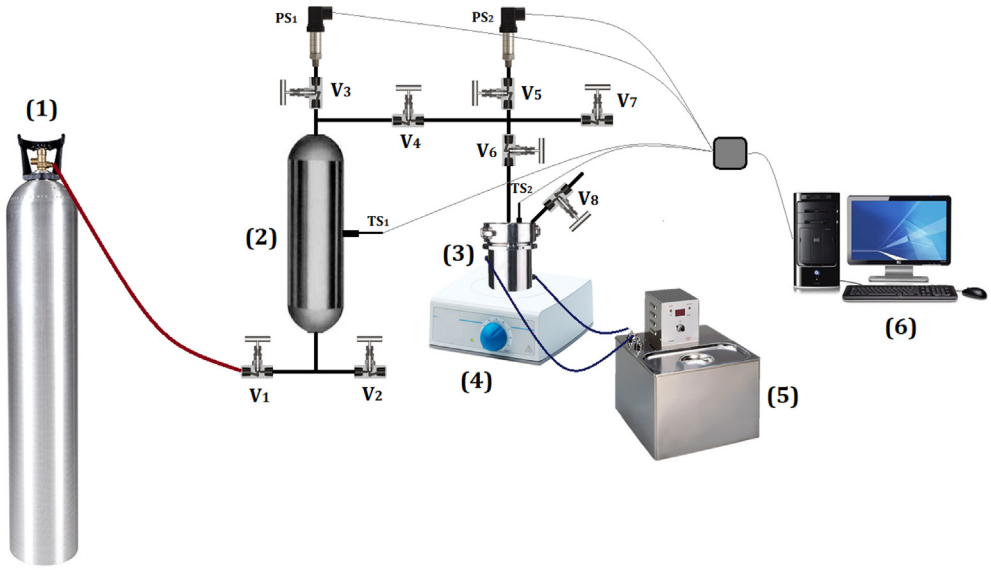

Fig. 2. Schematic of the experimental setup for CO_2 absorption; (1) CO_2 cylinder, (2) gas container (stainless steel, 182 ml) equipped with pressure sensor, PS_1 (Sensys, Model: M5156-11700X-050BG with the accuracy of ± 2.5 kPa) and temperature sensor, TS_1 (K-type with the accuracy of ± 0.1 K), (3) autoclave reactor (stainless steel, 37 ml) equipped with pressure sensor PS_2 (Sensys, Model: M5156-11700X-050BG with the accuracy of ± 2.5 kPa) and temperature sensor, TS_2 (K-type with the accuracy of ± 0.1 K), (4) magnetic stirrer (Fisher, Cat. No. 14–511-113), (5) circulating water bath (LAUDA Alpha RA 8, 248–373 K) and (6) computer.

solubility in BOLs. LJ-Global TPT2 is a newly developed perturbed-chain EoS in the framework of thermodynamic perturbation theory (TPT) for a fully flexible Lennard-Jones (LJ) chain systems introduced in Appendix A [26–28]. The chemical reaction equilibrium and phase equilibrium of CO_2 absorption in the selected BOLs are presented in Sections 4.3.1 and 4.2.3, respectively.

4. Results and discussion

4.1. Screening experiment

Screening experiments were conducted for DBU/alkanol/tertiary alkanol amine BOLs to determine the most appropriate solvent according to α_{eq} and α_R. First, the tertiary alkanolamines (DMEA, DEEA and MDEA) were examined with the fixed alcohol and DBU. Then, different alcohols were tested in conjunction with the chosen amine and DBU. In all the experiments the molar ratio of the components was kept constant at 1:1:1.

DMEA and DEEA (single-component CO_2-BOLs) are hybrid CO_2 absorbers at elevated pressures (6.9–34.5 bar) which can be regenerated upon depressurization [25]. Furthermore, it has been proven that MDEA/DBU mixture acts as a two-component SIL that produces alkylcarbonate salt after reaction with CO_2 [32]. Therefore, DMEA, DEEA and MDEA were chosen in the screening experiments to investigate the effect of tertiary alkanolamines in the three-component CO_2-BOLs.

Fig. 3 depicts the effect of tertiary alkanolamine type on the pressure drop of the reactor as a function of time in DBU-based CO_2-BOLs. The experiments were carried out at the temperature of 35.0 °C, the initial reactor pressure of 25.0 bar and equimolar mixtures of alcohol/base/amine using 1-hexanol as alcohol in all the experiments. Results show that DMEA exhibited higher α_R with the order of: DMEA > DEEA > MDEA. The maximum CO_2 loadings (α_{eq}) was obtained to be 0.436 using DEEA (inset of Fig. 3). However, the chosen tertiary alkanolamine was DMEA because of significantly higher absorption rate and more rapidly reaching to equilibrium in comparison to other amines (DEEA and MDEA) despite of slightly lower CO_2 loading in comparison to DEEA. The

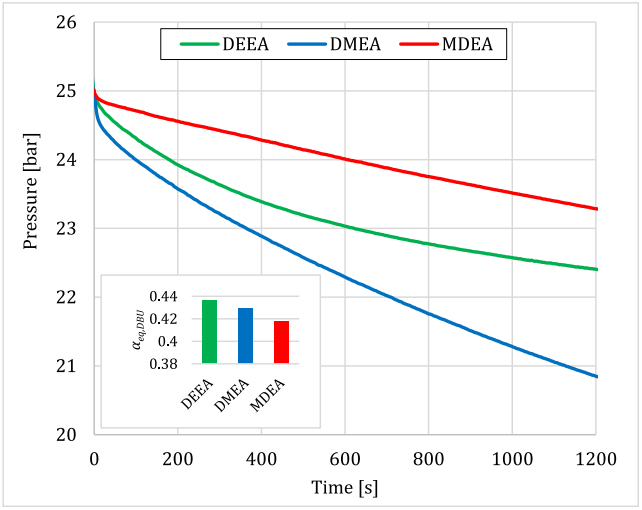

Fig. 3. The effect of tertiary alkanolamine on the CO_2 absorption rate from the initial pressure of 25.0 bar at the constant temperature of 35.0 °C using an equimolar mixture of DBU/1-hexanol/amine.

differences in CO_2 loading using various tertiary alkanolamines can be attributed to the basicity of amines and the stabilization of ionic species based on amine polarity before and after CO_2 uptake. DEEA is more basic than DMEA due to the more strongly electron donating substituents. The polarity of DMEA is higher than DEEA because of smaller substituents that leads to more efficient stabilization of the corresponding zwitterionic alkylcarbonate (Fig. 1). In contrary, higher polarity suppresses the physical absorption of CO_2 into the SILs [25].

The effect of alcohol in the DBU-based three-component BOLs comprised of equimolar (1:1:1) mixture of DBU, DMEA and alcohol (methanol, hexanol, n-butanol, *sec*-butanol and *tert*-butanol) at the fixed temperature of 35.0 °C and the initial reactor pressure of 25.0 bar is illustrated in Fig. 4. Among the evaluated alcohols, n-butanol had the highest α_R and α_{eq}.

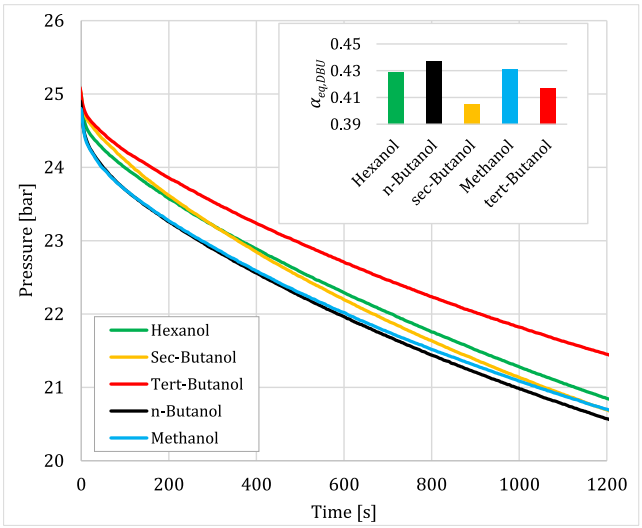

Fig. 4. The effect of alcohol type on the CO_2 absorption rate from the initial pressure of 25.0 bar at the constant temperature of 35.0 °C using an equimolar mixture of DBU/alcohol/DMEA.

The order of α_R and α_{eq} is as follows:

α_R: n-butanol > methanol > *sec*-butanol > hexanol > *tert*-butanol.

α_{eq}: n-butanol > methanol > hexanol > *tert*-butanol > *sec*-butanol.

Moreover, experiments showed that primary alcohols (methanol, n-butanol and hexanol) showed better performance in comparison to secondary (*sec*-butanol) and especially tertiary (*tert*-butanol) alcohols. The poorer performance of secondary and tertiary alcohols could be attributed to their steric hindrance that destabilizes the alkylcarbonate salts ($[BaseH^+][ROCO_2^-]$). The obtained results showed that the type of primary alcohols has negligible effect on the α_{eq} (α_{eq} = 0.429–0.437) compared to the effect of tertiary alkanolamines. The values of ΔG and ΔH of the CO_2 reaction with the two-component BOLs in the study of Heldebrant et al. [15] were almost independent of the alcohol type. However, the physical properties including viscosity and melting point can be tuned by changing the chain length of alcohols in the solvent mixture. Phan et al. [33] examined the melting point of two-component BOLs prepared from DBU and linear alcohols (methanol, ethanol, propanol, n-butanol, n-hexanol, n-octanol and n-decanal). They found that propylcarbonate and butylcarbonate salts had the lowest melting point (T_m < 283 K), which is advantageous for industrial applications. They also obtained inferior conversions using secondary and tertiary alcohols in comparison to primary alcohols. In Section 4.2, the mixture design approach is used to evaluate the effect of proportions of selected components (DBU, n-butanol and DMEA) on the equilibrium CO_2 absorption and absorption rate.

4.2. Mixture design approach

The mixture design approach [24], a special class of response surface methodology (RSM) [34] was chosen to investigate the influence of mole fraction of components in the three-component CO_2-BOLs (DBU/amine/alcohol). Statistical mixture design was applied for the design of experiments and modeling of α_{eq} and α_R based on the components proportion. Simplex lattice design (lattice degree = 3) was selected with 3 components including DBU, n-butanol (n-BuOH) and DMEA.

The experimental data for α_{eq} and α_R were fitted by the linear (Eq. (8)), quadratic (Eq. (9)), special cubic (Eq. (10)), full cubic (Eq. (11)) and special quartic (Eq. (12)) models and the best ones based on accuracy and simplicity were chosen.

$$Y = \sum_{i=1}^{q} \beta_i Z_i \tag{8}$$

$$Y = \sum_{i=1}^{q} \beta_i Z_i + \sum_{i\neq j}^{q} \beta_{ij} Z_i Z_j \tag{9}$$

$$Y = \sum_{i=1}^{q} \beta_i Z_i + \sum_{i\neq j}^{q} \beta_{ij} Z_i Z_j + \sum_{i\neq j\neq k}^{q} \beta_{ijk} Z_i Z_j Z_k \tag{10}$$

$$Y = \sum_{i=1}^{q} \beta_i Z_i + \sum_{i=1}^{q-1} \sum_{j>i}^{q} \beta_{ij} Z_i Z_j + \sum_{i\neq j\neq k}^{q} \beta_{ijk} Z_i Z_j Z_k + \sum_{i\neq j}^{q} \beta_{ij} Z_i Z_j (Z_i - Z_j) \tag{11}$$

$$Y = \sum_{i=1}^{q} \beta_i Z_i + \sum_{i=1}^{q-1} \sum_{j>i}^{q} \beta_{ij} Z_i Z_j + \sum_{i\neq j\neq k}^{q} \beta_{ijk} Z_i^2 Z_j Z_k \tag{12}$$

where, Y, Z_i, β_i and q are the estimated response, mole fraction of the ith component, coefficient of model and the number of components, respectively.

4.2.1. Evaluation of mixture design models for CO_2 absorption

Table 2 shows the obtained α_R and α_{eq} in the designed experiments. The coefficients of the full cubic equation (Eq. (11)) were calculated using the statistical mixture design approach. The regression coefficients and the analysis of variance (ANOVA) for the models of α_R and α_{eq} are presented in Tables 3 and 4, respectively.

The fitted models for α_R and α_{eq} were verified based on the p-values criteria ($p < 0.001$: highly significant, $0.001 \leq p < 0.05$: significant and $p \geq 0.05$: insignificant) via ANOVA. In the model for α_R the linear and full cubic terms were significant ($0.001 \leq p < 0.05$) while the quadratic and special cubic terms were insignificant ($p \geq 0.05$), albeit the full cubic interaction term of n-BuOH and DBU proportions ($B \times A \times (B\text{-}A)$) was significant (p = 0.019). In the case of α_{eq}, the linear and quadratic terms were obtained to be significant, but the cubic and special cubic terms were insignificant, though, the full cubic interaction term of DBU and DMEA proportions ($C \times B \times (C\text{-}B)$) was also significant (p = 0.025).

The models for α_{eq} (R^2 = 99.4% and $adj\text{-}R^2$ = 97.5%) and α_R (R^2 = 98.6% and $adj\text{-}R^2$ = 94.4%) as a function of component proportions are represented by Eqs. (13) and (14), respectively.

$$\begin{aligned}\alpha_{R.DBU} = {} & 0.3167C + 0.1405B + 0.1464A - 0.1815CB \\ & - 0.0374CA + 0.1390BA + 0.947CBA \\ & + 0.390CB(C - B) - 0.196CA(C - A) \\ & - 0.586BA(B - A)\end{aligned} \tag{13}$$

$$\begin{aligned}\alpha_{eq.DBU} = {} & 0.3606C + 0.2877B + 0.1577A + 0.6935CB \\ & + 0.0169CA + 1.0464BA - 1.025CBA \\ & - 0.605CB(C - B) - 0.165CA(C - A) \\ & + 0.311BA(B - A)\end{aligned} \tag{14}$$

Fig. 5.a shows the effect of component (DBU, DMEA and n-BuOH) proportions on the total CO_2 absorption (α_{eq}) at the fixed temperature of 35.0 °C and the initial pressure of 25.0 bar. Moreover, the number of absorbed CO_2 molecules per mol of solvent within 20 min at the above conditions (α_R) is illustrated in Fig. 5.b.

Table 2
Mixture design for α_R and α_{eq} and the observed responses.

Run Order	DMEA (*C*)	DBU (*B*)	n-BuOH (*A*)	α_{eq}(experiment)	α_{eq} (model)	α_R(experiment)	α_R(model)
1	0.667	0.333	0.000	0.444	0.445	0.248	0.246
2	0.000	0.667	0.333	0.495	0.499	0.127	0.130
3	0.333	0.000	0.667	0.252	0.241	0.216	0.209
4	0.167	0.167	0.667	0.302	0.323	0.224	0.241
5	0.667	0.000	0.333	0.279	0.284	0.236	0.237
6	0.000	1.000	0.000	0.289	0.287	0.142	0.140
7	0.000	0.000	1.000	0.157	0.157	0.147	0.146
8	0.000	0.333	0.667	0.421	0.410	0.225	0.218
9	0.333	0.333	0.333	0.437	0.425	0.241	0.227
10	0.333	0.667	0.000	0.510	0.510	0.129	0.130
11	1.000	0.000	0.000	0.362	0.360	0.318	0.316
12	0.167	0.667	0.167	0.503	0.503	0.125	0.128
13	0.667	0.167	0.167	0.361	0.360	0.260	0.266

Table 3
Regression coefficients and analysis of variance (ANOVA) for the predicted full-cubic model of α_R.

Source	DF	Coef	SE Coef	Seq SS	Adj SS	Adj MS	F-Value	T-Value	P-Value
Regression	9			0.045714	0.045714	0.005079	23.60		0.012
Linear	2			0.032842	0.020076	0.010038	46.64		0.005
C		0.3167	0.0146						
B		0.1405	0.0146						
A		0.1464	0.0146						
Quadratic	3			0.003471	0.003579	0.001193	5.54		0.097
$C \times B$	1	−0.1815	0.0654	0.000821	0.001655	0.001655	7.69	−2.77	0.069
$C \times A$	1	−0.0374	0.0654	0.000103	0.000070	0.000070	0.33	−0.57	0.608
$B \times A$	1	0.1390	0.0654	0.002547	0.000970	0.000970	4.51	2.12	0.124
Special Cubic	1			0.001060	0.001060	0.001060	4.92		0.113
$C \times B \times A$	1	0.947	0.427	0.001060	0.001060	0.001060	4.92	2.22	0.113
Full Cubic	3			0.008341	0.008341	0.002780	12.92		0.032
$C \times B\times$ *(C-B)*	1	0.390	0.125	0.002637	0.002081	0.002081	9.67	0.053	0.053
$C \times A\times$ *(C-A)*	1	−0.196	0.125	0.001007	0.000529	0.000529	2.46	0.215	0.215
$B \times A\times$ *(B-A)*	1	−0.586	0.125	0.004697	0.004697	0.004697	21.83	0.019	0.019
Residual Error	3			0.000646	0.000646	0.000215			
Total	12			0.046359					

Table 4
Regression coefficients and analysis of variance (ANOVA) for the predicted full-cubic model of α_{eq}.

Source	DF	Coef	SE Coef	Seq SS	Adj SS	Adj MS	F-Value	T-Value	P-Value
Regression	9			0.143214	0.143214	0.015913	54.77		0.004
Linear	2			0.061135	0.021181	0.010590	36.45		0.008
C		0.3606	0.0170						
B		0.2877	0.0170						
A		0.1577	0.0170						
Quadratic	3			0.073206	0.071205	0.023735	81.69		0.002
$C \times B$	1	0.6935	0.0760	0.016873	0.024170	0.024170	83.18	9.12	0.003
$C \times A$	1	0.0169	0.0760	0.001069	0.000014	0.000014	0.05	0.22	0.838
$B \times A$	1	1.0464	0.0760	0.055264	0.055030	0.055030	189.39	13.76	0.001
Special Cubic	1			0.001241	0.001241	0.001241	4.27		0.131
$C \times B \times A$	1	−1.025	0.496	0.001241	0.001241	0.001241	4.27	−2.07	0.131
Full Cubic	3			0.007631	0.007631	0.002544	8.75		0.054
$C \times B\times$ *(C-B)*	1	−0.605	0.146	0.006082	0.005007	0.005007	17.23	−4.15	0.025
$B \times A\times$ *(B-A)*	1	−0.165	0.146	0.000223	0.000373	0.000373	1.29	−1.13	0.339
$B \times A\times$ *(B-A)*	1	0.311	0.146	0.001327	0.001327	0.001327	4.57	2.14	0.122
Residual Error	3			0.000872	0.000872	0.000291			
Total	12			0.144086					

DBU does not chemically bind to CO_2 to produce a stable zwitterionic adduct [15]. Thus, CO_2 uptake into the DBU (α_{eq} = 0.157) is just due to the physical absorption and the production of bicarbonate salt because of small amounts of water in solvent.

DMEA as a single component BOL resulted in the equilibrium absorption of 0.362 mol CO_2/mol DMEA from 25.0 bar to the equilibrium pressure at 35.0 °C. Rainbolt et al. [25] calculated that the ratio of reacted DMEA with CO_2 (DMEA-CO_2 zwitterion) to the unreacted DMEA at 34.5 bar is about 1:3. Addition of DBU to DMEA led to the higher CO_2 loading due to the formation of alkylcarbonate salt ($[DBUH^+][(CH_3)_2NCH_2CH_2OCOO^-]$) such that the two-component BOL of DBU/DMEA with a molar ratio of 0.63:0.37 was capable to absorb 0.513 mol CO_2 per mol of solvent based on the mixture design model.

Addition of alcohol (n-BuOH) to the optimum mixture of DBU/DMEA (0.63:0.37) had two opposite effects. On one hand, increasing the amount of alcohol resulted in the lower α_{eq} (Fig. 5.a) because of lower DBU concentration. On the other hand, addition of alcohol enhanced the α_R (Fig. 5.b). Moreover, in the two-component BOL composed of alcohol and base, increasing the

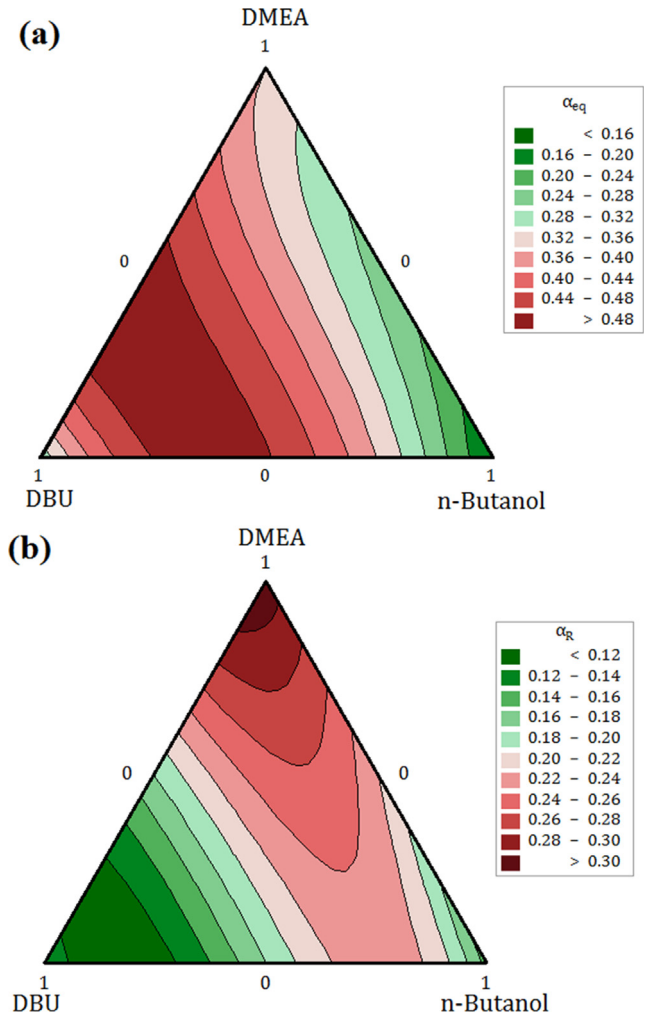

Fig. 5. The effect of component proportions on the (a) α_{eq} and (b) α_R in the DBU/DMEA/n-BuOH BOL at the initial pressure of 25.0 bar and the temperature of 35.0 °C.

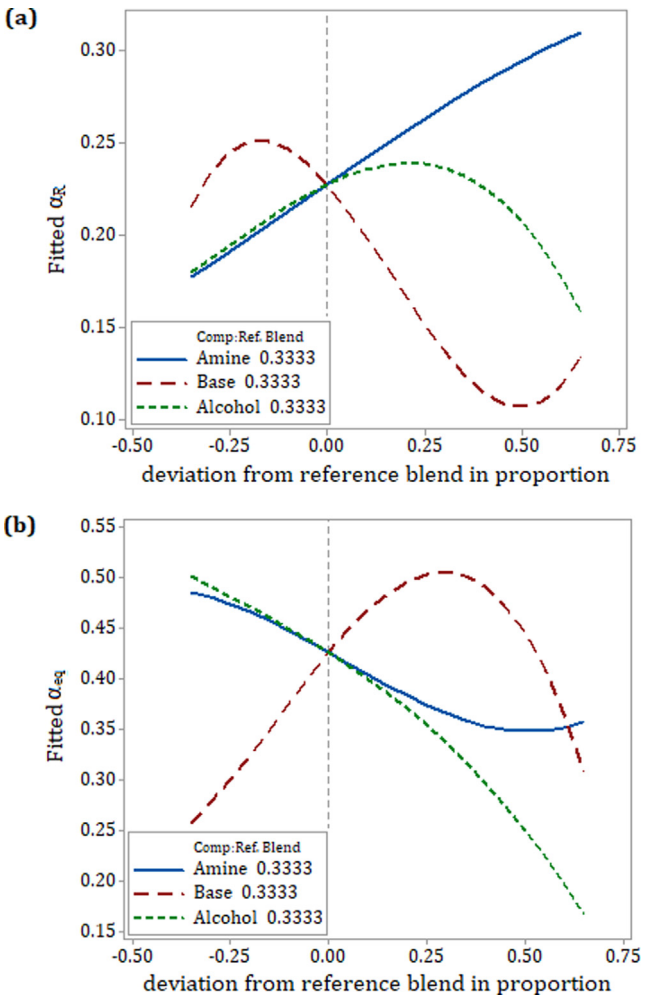

Fig. 6. Cox response trace plot for the effect of component proportions on the (a) α_R and (b) α_{eq} in the DBU/DMEA/n-BuOH BOL at the temperature of 35.0 °C and the initial CO_2 pressure of 25.0 bar.

alcohol proportion from 0 to the optimum value of 0.39 led to the α_{eq} = 0.502. But, more n-BuOH proportions decreased the CO_2 loading, whereas the CO_2 absorption rate was increased.

Cox response trace plots were also used to interpret effects of components on the α_R (Fig. 6.a) α_{eq} (Fig. 6.b):

- As the proportion of tertiary alkanolamine (DMEA) in the mixture increases (from 0 in equimolar n-BuOH/DBU SIL to 1 in pure DMEA), α_R increases such that the highest α_R of 0.318 mol CO_2/mol solvent was obtained using pure DMEA. Furthermore, decreasing the DMEA proportion in the reference blend, increases the CO_2 loading (α_{eq}), while higher DMEA proportions beyond the reference blend (0.333:0.333:0.333), decreases the CO_2 loading to a minimum value and then slightly increases.
- Increasing n-BuOH proportion in the three-component BOL from 0 in the equimolar DBU/DMEA BOL to about 0.59 enhances the CO_2 absorption rate, but at higher proportions the absorption rate reduces. Moreover, the addition of n-BuOH has a negative effect on the α_{eq} in all n-BuOH proportions.
- Increasing the DBU concentration from 0 in the equimolar DMEA/n-BuOH solvent leads to the more α_{eq} until the optimum proportion (≈0.63), but further addition of DBU decreases the α_{eq}. As the proportion of DBU in the reference blend increases, the absorption rate decreases until a minimum value. More DBU proportions (>0.82) has a positive effect on CO_2 absorption rate. As the DBU decreases in the reference blend, the dual counter effects of increase and decrease in α_{eq} is also observed.

4.3. Thermodynamic modeling

The results of screening experiments show that the equimolar mixture of DBU, DMEA and n-BuOH has the best performance for CO_2 uptake. Also, statistical mixture design approach shows that by considering both α_{eq} and α_R, the two-component and three-component BOLs with the DBU concentration of 0.1–0.2 have higher absorption efficiency. Therefore, DBU/n-BuOH (molar ratios: 0.1/0.9, 0.2/0.8 and 0.3/0.7), DBU/DMEA (molar ratios: 0.1/0.9 and 0.2/0.8) and DBU/DMEA/n-BuOH (molar ratios: 0.1/0.6/0.3 and 0.2/0.57/0.23) BOLs are chosen for thermodynamic modeling.

4.3.1. Chemical reaction equilibrium

The following chemical reactions take place in the liquid phase of DBU/n-BuOH (Eq. (15)), DBU/DMEA (Eqs. (20) and (21)) and DBU/DMEA/n-BuOH BOLs (Eqs. (26)–(29)) as a result of reaction with CO_2. Also the mass balance equations (Eqs. (16)–(19), (22)–(25) and (30)–(34)) for each solvent system are expressed below.

- DBU/n-BuOH BOL:

$$DBU + n-BuOH + CO_2 \overset{K_1}{\rightleftharpoons} IL_1([DBUH^+][n-BuOCOO^-]) \quad (15)$$

$$n^t_{n-BuOH} = n^e_{n-BuOH} + n^e_{IL_1} \quad (16)$$

$$n^t_{DBU} = n^e_{DBU} + n^e_{IL_1} \quad (17)$$

$$n^t_{CO_2} = n^{physical}_{CO_2} + n^e_{IL_1}(orn^{chemical}_{CO_2}) \quad (18)$$

$$n^e_{n-BuOH} + n^e_{DBU} + n^{physical}_{CO_2} + n^e_{IL_1} = n^e_t \quad (19)$$

- DBU/DMEA BOL:

$$DBU + DMEA + CO_2 \overset{K2}{\rightleftharpoons} IL_2([DBUH^+][DMEACOO^-]) \quad (20)$$

$$DMEA + CO_2 \overset{K_3}{\rightleftharpoons} IL_3(DMEA^+COO^-) \quad (21)$$

$$n^t_{DMEA} = n^e_{DMEA} + n^e_{IL_2} + n^e_{IL_3} \quad (22)$$

$$n^t_{DBU} = n^e_{DBU} + n^e_{IL_2} \quad (23)$$

$$n^t_{CO_2} = n^{physical}_{CO_2} + n^e_{IL_2} + n^e_{IL_3} \quad (24)$$

$$n^e_{DMEA} + n^e_{DBU} + n^{physical}_{CO_2} + n^e_{IL_2} + n^e_{IL_3} = n^e_t \quad (25)$$

- DBBU/DMEA/n-BuOH BOL:

$$DBU + n-BuOH + CO_2 \overset{K_1}{\rightleftharpoons} IL_1([DBUH^+][n-BuOCOO^-]) \quad (26)$$

$$DBU + DMEA + CO_2 \overset{K_2}{\rightleftharpoons} IL_2([DBUH^+][DMEACOO^-]) \quad (27)$$

$$DMEA + CO_2 \overset{K_3}{\rightleftharpoons} IL_3(DMEA^+COO^-) \quad (28)$$

$$DMEA + n-BuOH + CO_2 \overset{K_4}{\rightleftharpoons} IL_4([DMEAH^+][n-BuOO^-]) \quad (29)$$

$$n^t_{DMEA} = n^e_{DMEA} + n^e_{IL_2} + n^e_{IL_3} + n^e_{IL_4} \quad (30)$$

$$n^t_{DBU} = n^e_{DBU} + n^e_{IL_1} + n^e_{IL_2} \quad (31)$$

$$n^t_{CO_2} = n^{physical}_{CO_2} + n^e_{IL_1} + n^e_{IL_2} + n^e_{IL_3} + n^e_{IL_4} \quad (32)$$

$$n^t_{n-BuOH} = n^e_{n-BuOH} + n^e_{IL_1} + n^e_{IL_4} \quad (33)$$

$$n^e_{DMEA} + n^e_{DBU} + n^e_{n-BuOH} + n^{physical}_{CO_2} + n^e_{IL_1} + n^e_{IL_2} + n^e_{IL_3} + n^e_{IL_4} = n^e_t \quad (34)$$

The equilibrium constant of reactions is represented as [35].

$$K_j = \prod (x_i\gamma_i)^{\vartheta_{i,j}} = \exp(A^{(1)}_j + \frac{A^{(1)}_j}{T} + A^{(3)}_j \ln(T)) \quad (35)$$

where K_j, x_i, γ_i, v_i and T are the chemical equilibrium constant of reaction j based on mole fraction, mole fraction, activity coefficient, reaction stoichiometry of species i in reaction j and the absolute temperature, respectively.

The unsymmetrical activity coefficient (Eq. (36)) with the reference state of infinite dilution in solvent is applied for CO_2, while for other molecular and ionic species; the activity coefficient is defined by Eq. (37).

$$\gamma^*_{CO_2} = \frac{\varphi_{CO_2}(T,P,x_{CO_2})}{\varphi^{\infty}_{CO_2}(T,P,x_{CO_2}\to 0)} \quad (36)$$

$$\gamma_i = \frac{\varphi_i(T,P,x_i)}{\varphi^o_i(T,P,x_i\to 1)} \quad (37)$$

where φ, x and P are fugacity coefficient calculated by the LJ-Global TPT2, mole fraction and pressure, respectively. Also, the superscript 0 shows the reference standard state.

The equilibrium concentrations of all the molecular and ionic species in the liquid phase for each system are calculated by simultaneously solving the system of nonlinear equations due to chemical equilibrium reactions and mole balance equations. In the DBU/n-BuOH BOL, there is one equation due to chemical equilibrium constant as presented by Eq. (35) for the chemical equilibrium reaction (15). This equation and Eqs. (16)–(19) are solved simultaneously to find 5 unknowns including 4 number of moles of components in equilibrium (n^e_{1-BuOH}, n^e_{DBU}, $n^{physical}_{CO_2}$ and $n^e_{IL_1}$) and the total number of moles of components in the liquid phase at equilibrium (n^e_t). In the case of DBU/DMEA BOL, 6 equations (Eqs. (21)–(25) and the equation of chemical equilibrium constant of reaction (20)) are solved simultaneously to obtain 6 unknowns including: n^e_{DMEA}, n^e_{DBU}, $n^{physical}_{CO_2}$, $n^e_{IL_2}$, $n^e_{IL_3}$ and n^e_t. Chemical equilibrium constant equations due to reactions (26)–(29) and Eqs. (30)–(34) are also used to determine 9 unknown quantities of: n^e_{DMEA}, n^e_{DBU}, n^e_{1-BuOH}, $n^{physical}_{CO_2}$, $n^e_{IL_1}$, $n^e_{IL_2}$, $n^e_{IL_3}$, $n^e_{IL_4}$ and n^e_t in the DBU/DMEA/n-BuOH system.

4.3.2. Phase equilibrium

Vapor-liquid equilibrium (VLE) calculation is carried out by the φ-φ approach using LJ-Global TPT2 EoS [26]. The presence of DBU and DMEA in the vapor phase was ignored due to their low vapor pressure in the temperature range of this study (i.e. 25.0, 35.0 and 45.0 °C). Thus, only CO_2 and n-BuOH molecules are present in the vapor phase. Also, all the ionic species exist in liquid phase. The phase equilibrium equations are presented as follows.

$$x_i\varphi^l_i = y_i\varphi^v_i i = H_2O, CO_2 \quad (38)$$

where y_i is the mole fraction of species i in the vapor phase and superscript l and v denote for liquid and vapor phases, respectively. As mentioned before the fugacity coefficient of all molecular and ionic species in liquid and vapor phases are calculated by LJ-Global TPT2 EoS [26].

4.3.3. Pure component parameters

The properties of pure associating compounds are described by LJ-Global TPT2 EoS. The parameters of the EoS are: chain length (m), segment size (σ), segment energy (ε), the volume of association ($\kappa^{A_iB_j}$) and the energy of association ($\varepsilon^{A_iB_j}$). The first three parameters are only required to describe the non-associating compounds. The adjustable parameters for each molecule were regressed by simultaneous fitting the saturated liquid density and vapor pressure using the following objective function (OF).

$$OF = \sum_{i=1}^{n}\left|\frac{P^{sat}_{i,calc} - P^{sat}_{i,exp}}{P^{sat}_{i,exp}}\right| + \sum_{i=1}^{n}\left|\frac{\rho^l_{i,calc} - \rho^l_{i,exp}}{\rho^l_{i,exp}}\right| \quad (39)$$

where P^{sat} and ρ^l are the vapor pressure and the saturated liquid density, respectively. The results of fitting the EoS parameters are presented in Table 5 for CO_2, n-BuOH, DMEA and DBU. 2B association scheme was chosen for all associating compounds.

Table 5
Pure component parameters of LJ-Global TPT2 EoS.

Molecular species	m	σ (Å)	ε/k (K)	$\kappa^{A_iB_j}$	$\varepsilon^{A_iB_j}/k$ (K)	AAD%*AAD%*		Reference of data
						P^{sat}	ρ^{l}	
CO_2	2.5012	2.6234	160.73	-	-	2.94	4.80	[36]
DBU	3.6525	3.9329	383.59	-	-	1.53	0.34	[37–40]
n-BuOH	2.2912	3.9621	186.48	0.008385	2601.7	1.86	0.94	[41,42]
DMEA	2.9362	3.3116	224.95	0.033177	2645.4	2.11	1.36	[43–45]
Ionic species	m	σ (Å)	ε/k (K)	$\kappa^{A_iB_j}$	$\varepsilon^{A_iB_j}/k$ (K)			
IL1	11.4587	3.3392	335.7	0.039173	1307.5			
IL2	11.7446	3.2418	374.5	0.054554	1512.1			
IL3	6.3317	3.1720	203.65	0.001251	1072.0			
IL4	10.8624	3.1772	310.7	0.040186	1651.9			

4.3.4. Binary molecular interaction parameters

Before modeling CO_2 solubility in two-component (DBU/n-BuOH and DBU/DMEA) and three-component (DBU/DMEA/n-BuOH) BOLs, the DBU/CO_2 and n-BuOH/CO_2 binary subsystems were studied. The binary interaction parameter (BIP) of n-BuOH/CO_2 binary system was adjusted using the experimental CO_2 solubility data

Table 6
Comparison between the experimental and calculated total CO_2 pressure in the two-component DBU/n-BuOH BOL at the temperatures of 25.0, 35.0 and 45.0 °C using the DBU mole fractions of 0.1, 0.2 and 0.3.

DBU mole fraction	T (°C)	α (mol CO_2/mol Solvent) ± uncertainty	P (bar) (experiment)	P (bar) (calculated)	AD%
0.1	25.0	0.098 ± 0.007	1.9	2.6	35.5
		0.110 ± 0.006	3.7	4.4	18.5
		0.129 ± 0.004	6.8	6.5	4.9
		0.150 ± 0.003	10.0	9.1	9.1
		0.200 ± 0.002	17.1	16.1	5.4
		0.265 ± 0.002	25.6	27.7	8.2
	35.0	0.102 ± 0.007	2.7	3.2	17.9
		0.116 ± 0.005	5.3	5.2	0.3
		0.139 ± 0.003	9.5	8.7	8.4
		0.173 ± 0.003	15.1	14.1	6.3
		0.240 ± 0.002	25.1	25.7	2.4
	45.0	0.106 ± 0.006	3.2	3.6	14.2
		0.116 ± 0.005	5.1	5.4	6.2
		0.131 ± 0.003	8.0	8.1	1.4
		0.152 ± 0.003	12.3	11.9	3.3
		0.178 ± 0.002	17.5	16.5	5.6
		0.226 ± 0.002	25.7	24.9	3.4
0.2	25.0	0.213 ± 0.009	5.0	5.9	17.3
		0.228 ± 0.008	7.4	7.8	4.7
		0.263 ± 0.005	12.7	12.2	3.6
		0.322 ± 0.003	20.6	19.7	4.4
		0.408 ± 0.002	31.1	30.3	2.7
		0.504 ± 0.002	40.2	41.8	3.9
	35.0	0.207 ± 0.009	4.1	4.7	15.0
		0.223 ± 0.009	7.1	7.2	0.3
		0.250 ± 0.006	11.6	11.4	1.4
		0.283 ± 0.004	17.0	16.6	2.4
		0.319 ± 0.003	23.0	22.4	2.3
		0.384 ± 0.003	31.9	33.3	4.4
	45.0	0.191 ± 0.008	3.4	3.9	16.9
		0.193 ± 0.010	3.7	4.2	15.1
		0.203 ± 0.009	5.4	5.9	9.0
		0.217 ± 0.009	8.1	8.0	1.4
		0.237 ± 0.007	12.1	11.2	7.4
		0.269 ± 0.004	18.0	16.3	9.4
		0.327 ± 0.003	27.9	25.6	8.3
0.3	25.0	0.311 ± 0.005	5.2	5.9	14.1
		0.361 ± 0.003	12.4	12.3	0.3
		0.422 ± 0.002	20.9	20.3	3.0
		0.549 ± 0.002	34.5	37.3	8.1
		0.590 ± 0.001	39.4	42.9	8.8
	35.0	0.285 ± 0.007	2.3	2.8	23.6
		0.319 ± 0.005	7.8	7.5	3.8
		0.361 ± 0.003	15.3	13.6	10.6
		0.415 ± 0.003	24.1	22.1	8.4
		0.502 ± 0.002	35.0	37.0	5.6
	45.0	0.235 ± 0.009	0.4	0.2	42.6
		0.326 ± 0.004	12.0	12.0	0.3
		0.380 ± 0.003	21.4	19.4	9.2
		0.505 ± 0.002	36.6	38.3	4.5
AAD%					8.5

[46–48]. Also, the BIP of DBU/CO_2 system was tuned using the Ostonen et al. [37] solubility data. BIPs are considered to be temperature dependent based on Eq. (40) and optimized using Eq. (41) as the OF.

$$k_{ij} = a + b/T \tag{40}$$

$$\mathrm{OF} = \sum_{i=1}^{n} \left| \frac{P_{i,calc}^{sat} - P_{i,exp}^{sat}}{P_{i,exp}^{sat}} \right| \tag{41}$$

The BIPs for n-BuOH/CO_2 and DBU/CO_2 systems were calculated to be as follows.

$$k_{n-BuOH-CO_2} = -0.2436 + 92.6240/T \tag{42}$$

$$k_{DBU-CO_2} = 0.1823 - 43.8393/T \tag{43}$$

The AAD%, in evaluating the total pressure are 11.23% and 5.21% for n-BuOH/CO_2 and DBU/CO_2 systems, respectively.

$$\mathrm{AAD}(\%) = \sum_{i=1}^{n} \left| \frac{Y_{i,calc}^{sat} - Y_{i,exp}^{sat}}{Y_{i,exp}^{sat}} \right| \times 100 \tag{44}$$

4.3.5. Modeling of CO_2 solubility in CO_2-BOLs

Tables 6-8 show the obtained experimental data in this work which are then used to model the CO_2 solubility in two-component (DBU/n-BuOH, DBU/DMEA) and three-component (DBU/DMEA/n-BuOH) CO_2-BOLs. As mentioned before modeling was carried out by simultaneous VLE and chemical equilibrium calculations using the φ-φ approach by applying LJ-Global TPT2 EoS to both liquid and vapor phases. Three groups of parameters are adjusted using the CO_2 solubility data in CO_2-BOLs: (1) the binary interaction parameters (BIPs), (2) the parameters of LJ-Global TPT2 EoS for the produced ionic spices and (3) the equilibrium constants of reactions.

The reactive bubble pressure calculation algorithm (Appendix B) is employed for parameter optimization. The algorithm consists of two main loops: (a) in the inner loop the chemical equilibrium and mass balance equations are solved simultaneously to obtain the mole fraction of molecular and ionic species at the given CO_2 loading and temperature in the liquid phase. (b) in the outer loop the VLE calculation is carried out to determine the bubble point pressure and mole fraction of n-BuOH and CO_2 in the vapor phase.

The liquid phase of CO_2 reaction with DBU/DMEA/n-BuOH contains eight molecular and ionic species. Table 9 illustrates that 64 BIPs exist in this system. Two assumptions have been made to reduce the number of adjustable parameters: (1) The interaction between ionic species and the molecules are neglected and (2) the interaction between ionic liquids with the same anion and same cation was ignored. The BIPs are adjusted by optimization of the bubble point pressure data of the DBU/n-BuOH, DBU/DMEA and DBU/DMEA/n-BuOH solvent systems using the same OF as Eq. (40) where the number of fitted parameters are only 2, 6 and 8, respectively.

To the best of our knowledge, no data is reported for the equilibrium constants of the reactions present in this work, hence, they are all treated as adjustable parameters. The adjusted parameters including: LJ-Global TPT2 EoS parameters (IL_1 adjusted by DBU/n-BuOH data, IL_2 and IL_3 by DBU/DMEA data and IL_4 by DBU/DMEA/n-BuOH data), BIPs, and equilibrium constants (K_1 adjusted by DBU/n-BuOH data, K_2 and K_3 by DBU/DMEA data and K_4 by DBU/DMEA/n-BuOH data) are presented in Tables 5, 9 and 10, respectively.

Table 7
Comparison between the experimental and calculated total CO_2 pressure in the two-component DBU/DMEA BOL at the temperatures of 25.0, 35.0 and 45.0 °C using the DBU mole fractions of 0.1 and 0.2.

DBU mol fraction	T (°C)	α (mol CO_2/mol Solvent) ± uncertainty	P (bar) (experiment)	P (bar) (calculated)	AD%
0.1	25.0	0.161 ± 0.009	3.2	4.3	33.2
		0.233 ± 0.007	7.2	7.7	7.1
		0.329 ± 0.004	13.6	13.0	4.5
		0.439 ± 0.003	22.2	20.0	9.9
		0.552 ± 0.003	31.3	28.0	10.3
	35.0	0.144 ± 0.010	3.8	4.8	25.7
		0.190 ± 0.010	7.4	8.0	8.1
		0.285 ± 0.005	15.2	14.8	3.0
		0.406 ± 0003	25.4	23.3	8.0
		0.516 ± 0.002	33.7	31.0	7.9
		0.592 ± 0.002	38.7	36.2	6.4
	45.0	0.146 ± 0.010	5.7	6.6	15.0
		0.206 ± 0.009	11.9	11.8	0.6
		0.290 ± 0.005	20.7	19.4	6.2
		0.383 ± 0.003	29.6	28.2	4.6
		0.462 ± 0.003	37.0	36.0	2.9
0.2	25.0	0.224 ± 0.007	2.9	1.9	34.4
		0.280 ± 0.005	6.8	6.5	4.9
		0.372 ± 0.003	14.0	14.2	1.4
		0.482 ± 0.002	22.6	23.6	4.4
		0.600 ± 0.001	32.1	33.8	5.5
	35.0	0.221 ± 0.007	3.9	4.5	17.5
		0.253 ± 0.006	6.8	7.0	3.1
		0.307 ± 0.004	12.0	11.4	5.7
		0.376 ± 0.004	19.1	17.1	10.7
		0.465 ± 0.003	27.6	24.7	10.5
		0.581 ± 0.002	37.9	35.1	7.3
	45.0	0.176 ± 0.009	1.4	1.6	20.9
		0.205 ± 0.008	4.1	4.3	5.9
		0.241 ± 0.007	8.3	7.8	5.8
		0.303 ± 0.004	14.7	14.0	4.8
		0.381 ± 0.003	24.1	21.9	9.2
		0.501 ± 0.002	35.3	34.8	1.5
		0.558 ± 0.002	40.9	41.2	0.7
AAD%					5.8

Table 8
Comparison between the experimental and calculated total CO_2 pressure in the three-component DBU/DMEA/n-BuOH BOL at the temperatures of 25.0, 35.0 and 45.0 °C using the DBU mole fractions of 0.1 and 0.2.

DBU mol fraction	T (°C)	α (mol CO_2/mol Solvent) ± uncertainty	P (bar) (experiment)	P (bar) (calculated)	AD%
0.1	25.0	0.161 ± 0.010	3.4	4.4	30.0
		0.224 ± 0.008	7.2	8.0	12.0
		0.267 ± 0.007	10.3	10.6	3.2
		0.334 ± 0.004	15.5	14.9	4.0
		0.356 ± 0.004	17.4	16.4	5.7
		0.441 ± 0.003	24.2	22.3	7.9
		0.572 ± 0.002	35.4	32.2	8.8
	35.0	0.114 ± 0.011	1.8	2.1	17.5
		0.126 ± 0.011	2.7	3.0	9.9
		0.141 ± 0.010	3.9	4.1	5.1
		0.157 ± 0.010	5.3	5.5	3.0
		0.186 ± 0.009	7.6	7.7	1.2
		0.206 ± 0.009	9.1	9.3	2.9
		0.235 ± 0.008	11.9	11.7	1.6
		0.256 ± 0.007	14.0	13.5	3.9
		0.284 ± 0.006	16.8	15.8	6.2
		0.323 ± 0.006	20.8	19.1	8.0
		0.370 ± 0.004	25.3	23.3	7.9
		0.424 ± 0.003	31.0	28.2	9.3
		0.527 ± 0.002	39.9	37.8	5.4
		0.565 ± 0.002	43.3	41.5	4.2
	45.0	0.102 ± 0.013	2.0	1.5	25.6
		0.119 ± 0.012	3.6	3.2	10.9
		0.143 ± 0.011	6.2	5.7	8.9
		0.165 ± 0.010	8.7	8.1	7.5
		0.206 ± 0.009	12.6	12.3	2.3
		0.248 ± 0.007	17.7	16.7	6.0
		0.325 ± 0.005	26.4	24.9	5.7
		0.418 ± 0.003	34.7	34.7	0.1
		0.478 ± 0.003	40.7	41.2	1.3
		0.524 ± 0.002	44.0	46.3	5.2
0.2	25.0	0.214 ± 0.008	2.2	0.6	73.2
		0.257 ± 0.007	5.5	4.5	18.1
		0.305 ± 0.005	9.6	8.9	7.4
		0.376 ± 0.003	15.8	15.4	2.6
		0.466 ± 0.002	23.7	23.5	0.7
		0.615 ± 0.002	35.5	37.1	4.5
	35.0	0.214 ± 0.009	2.9	3.8	31.9
		0.224 ± 0.008	3.9	4.8	21.0
		0.235 ± 0.008	5.3	5.9	12.0
		0.252 ± 0.007	7.0	7.5	7.4
		0.266 ± 0.007	8.5	8.9	5.1
		0.285 ± 0.006	10.6	10.8	1.8
		0.310 ± 0.005	13.6	13.3	2.4
		0.343 ± 0.004	17.2	16.5	3.9
		0.360 ± 0.004	19.3	18.3	5.6
		0.378 ± 0.003	21.3	20.0	6.1
		0.397 ± 0.003	23.1	22.0	4.9
		0.426 ± 0.003	25.7	24.9	3.3
		0.445 ± 0.002	28.6	26.9	5.8
		0.473 ± 0.002	31.4	29.8	5.1
		0.496 ± 0.002	34.7	32.2	7.3
		0.526 ± 0.002	38.5	35.2	8.5
	45.0	0.170 ± 0.011	1.6	1.0	36.4
		0.185 ± 0.010	2.9	3.0	0.7
		0.203 ± 0.009	4.8	5.3	9.7
		0.220 ± 0.009	7.1	7.5	5.5
		0.241 ± 0.008	9.9	10.2	3.3
		0.267 ± 0.007	13.3	13.5	1.6
		0.299 ± 0.005	17.6	17.8	1.0
		0.346 ± 0.004	23.8	24.0	0.8
		0.409 ± 0.003	31.6	32.5	2.6
		0.495 ± 0.002	41.0	44.3	8.0
AAD%					8.6

Tables 6-8 show the results of calculating the total pressure as a function of CO_2 loading at different temperatures and concentrations for DBU/n-BuOH, DBU/DMEA and DBU/DMEA/n-BuOH BOLs, respectively. As can be seen, the AAD% values for calculation of bubble point pressure for DBU/n-BuOH, DBU/DMEA and DBU/DMEA/n-BuOH BOLs are 8.5%, 5.8% and 8.6%, respectively.

Figs. 7-9 show the comparison between the experimental and calculated total pressure against CO_2 loading for the DBU/n-BuOH, DBU/DMEA and DBU/DMEA/n-BuOH BOLs, respectively. It is observed that the results of modeling are in a good agreement with the experimental data such that similar trends were obtained for CO_2 loading.

Table 9
The BIPs considered in the LJ-Global TPT2 EoS for the solubility of CO_2 in DBU/DMEA/n-BuOH solvent system.

IL_4	IL3	IL_2	IL_1	CO_2	n-BuOH	DMEA	DBU	component
0.0915	0.1615			Eq. (43)	0.06479	0.1025	0	DBU
			0.1833	0.1123	0.1537	0	0.1025	DMEA
	0.0975	0.1454		Eq. (42)	0	0.1537	0.06479	n-BuOH
0.0121	0.0327	0.0121	0.04966	0	Eq. (42)	0.1123	Eq. (43)	CO_2
	0.1523		0	0.04966		0.1833		IL_1
0.1217	0.0076	0		0.0121	0.1454			IL_2
	0	0.0076	0.1523	0.0327	0.0975		0.1615	IL3
0		0.1217		0.0121			0.0915	IL_4

Table 10
Coefficients of chemical reaction equilibrium constants introduced in Eq. (35).

$A^{(3)}$	$A^{(2)}$	$A^{(1)}$	Equilibrium Constant
1.009	0.3878	−0.04224	K_1
−70.79	−20680	477	K_2
−62.56	−18580	418.7	K_3
−31.61	−8675	212.2	K_4

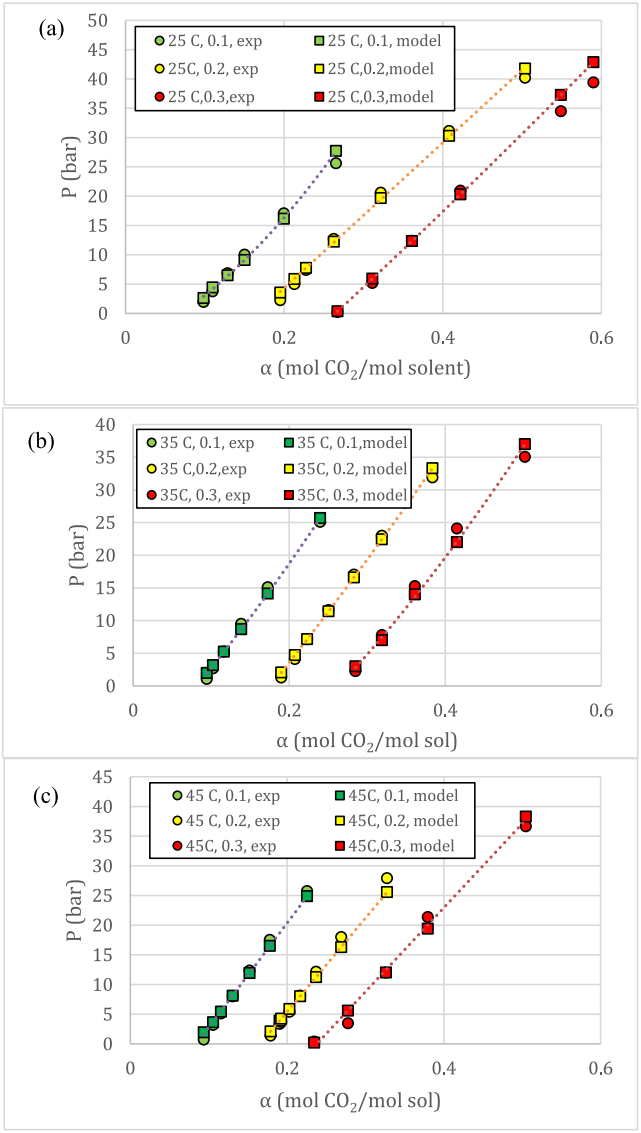

Fig. 7. CO_2 loading (α) as a function of total pressure at (a) T = 25.0 °C, (b) T = 35.0 °C and (c) T = 45.0 °C.

The results of equilibrium CO_2 solubility data and the thermodynamic modeling demonstrate that the two-component DBU/DMEA (0.1/0.9) BOL has higher CO_2 absorption capacity compared to the three-component DBU/DMEA/n-BuOH BOL (0.1/0.6/0.3). Similar outcome was also observed in the mixture design experiments. However, addition of small amounts of n-BuOH has positive effect on the CO_2 absorption rate. Increasing temperature at the fixed total pressure leads to lower CO_2 loading in all the solvents. Moreover, higher DBU concentration resulted in enhanced CO_2 absorption in all three studied BOLs due to the formation of more ionic liquids.

The obtained equilibrium constants in Table 10 can be used to determine the preference of CO_2 in the competitive reactions in the three-component solvent mixture. The equilibrium constants showed that CO_2 reacts more favorably with DBU/n-BuOH (Eq. (26)) in the following order: DBU/n-BuOH > DBU/DMEA (Eq. (27)) > DMEA/BuOH (Eq. (29)) > DMEA (Eq. (28)). The more acidic molecule, n-BuOH, binds stronger than DMEA to DBU and CO_2 to produce IL_1. Also, DBU as the more basic component has preference over DMEA in the reaction with n-BuOH and CO_2. The lowest equilibrium constant was observed for the direct reaction of CO_2 with DMEA to produce zwitterionic alkylcarbonate salt (IL_3).

5. Conclusions

The three-component switchable ionic liquids (or CO_2-binding organic liquids) as green solvents bring the higher degree of tunability for CO_2 capture. In this study, the DBU-based (DBU-tertiary alkanol amine-alcohol) CO_2-BOLs that produce alkylcarbonate salts upon reaction with CO_2 were synthesized. Production of alkyl carbonate salt is advantageous in term of solvent regeneration efficiency compared to alkyl carbamate salt. Introducing the superbase to the tertiary alkanol amines (single-component BOLs) enhances the CO_2 absorption capacity due to the formation of more ionic liquids. Moreover, the addition of alcohol to the two-component BOL (base/amine) enhances the CO_2 absorption rate. Also, addition of tertiary alkanol amines to the two-component BOLs (base/alcohol) allows the design of a pressure-sensitive solvent for efficient regeneration step. In this way, one can select the desired mixture proportions to produce SILs based on the required application. Screening experiments and statistical mixture design approach were used to investigate the effect of components type and concentration on the CO_2 absorption loading and absorption rate. The results showed that DMEA and n-BuOH had the best performance in DBU based BOLs for CO_2 absorption. The presented BOLs in this study combined the unique properties of two-component BOLs (alcohol/base) and single-component BOLs (tertiary alkanolamines) which led to the higher CO_2 absorption rate and capacity. As a result, these novel solvents can be used in the gas sweetening industries, greenhouse gas removal and especially in the separation processes where the chemicals are sensitive to water.

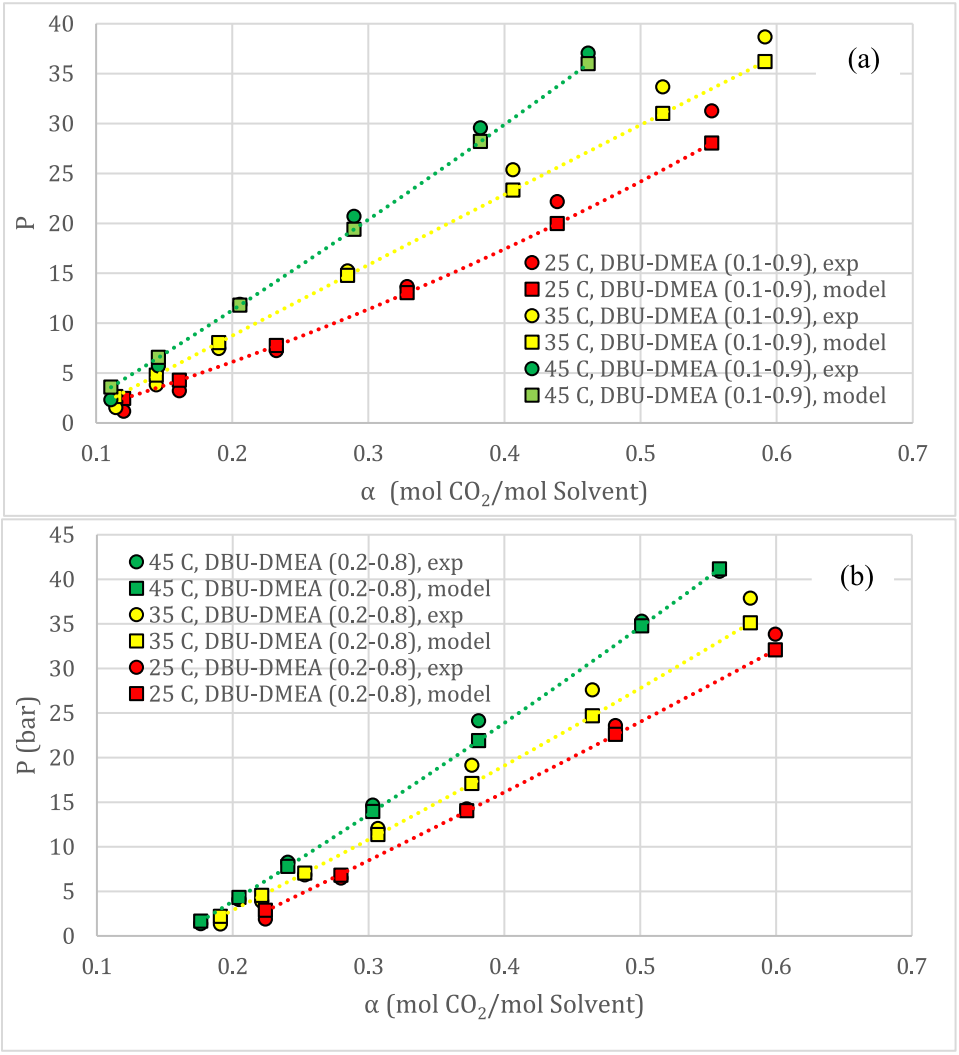

Fig. 8. CO_2 loading (α) as a function of total pressure using (a) DBU/DMEA (0.1/0.9) and (b) DBU/DMEA (0.2/0.8).

For the first time, the experimental CO_2 solubility data were obtained for the DBU/n-BuOH, DBU/DMEA and DBU/DMEA/n-BuOH BOLs at three temperatures of 25.0, 35.0 and 45.0 °C. The mole fraction of DBU was chosen to be 0.1, 0.2 and 0.3 in the solvent mixture. Thermodynamic modeling of CO_2 solubility in the BOLs was successfully carried out using the LJ-Global TPT2 EoS by applying the φ-φ approach. Binary interaction parameters, equilibrium constants and LJ-Global TPT2 EoS parameter of the ILs were adjusted using the reactive bubble pressure calculation. The AAD% of DBU/n-BuOH, DBU/DMEA and DBU/DMEA/n-BuOH BOLs were determined to be 8.5%, 5.8% and 8.6%, respectively.

CRediT authorship contribution statement

Ali Hedayati: Conceptualization, Methodology, Validation, Formal analysis, Investigation, Writing - original draft, Visualization. **Farzaneh Feyzi:** Resources, Writing - review & editing, Supervision, Project administration, Funding acquisition.

Declaration of Competing Interest

The authors declare that they have no known competing financial interests or personal relationships that could have appeared to influence the work reported in this paper.

Acknowledgments

The financial support provided by Iran National Science Foundation (grant number: 97011809) is gratefully acknowledged.

Appendix A

The residual Helmholtz energy for the LJ-Global TPT2 EoS is represented as:

$$\frac{A_{res}}{NkT} = \frac{A_{res}^{RC}}{NkT} + \frac{A_{res}^{disp}}{NkT} + \frac{A_{res}^{ass}}{NkT} \tag{A1}$$

A, N, k and *T* are the molar Helmholtz energy, the Avogadro's number, the Boltzmann's constant and the temperature, respectively. Superscript RC, disp, and ass stand for repulsive chain, dispersion and association, respectively.

Each of the terms of EoS are described below:

- *The repulsive chain term*:

$$\frac{A_{res}^{RC}}{NkT} = m\frac{A_{res}^{WCA}}{N^{WCA}kT} - (m-1)\ln y^{WCA}(\sigma) + \ln\left[\left(\frac{c-1}{2\xi(1-m^{-2})}\right)^{m}\left(\frac{1-m^{-1}}{c-m^{-1}}\right)(1+4\xi)\right] \tag{A2}$$

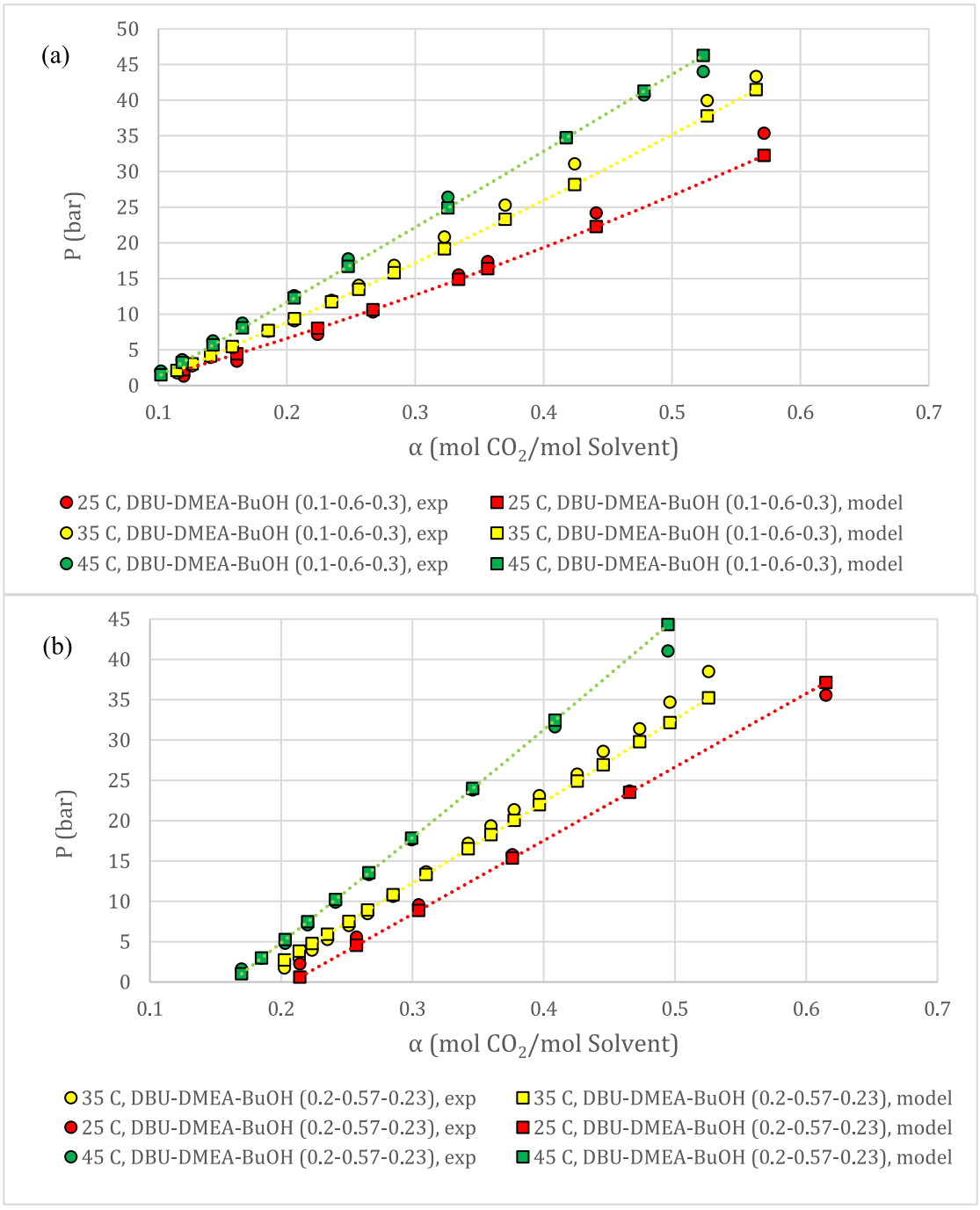

Fig. 9. CO_2 loading (α) as a function of total pressure using (a) DBU/DMEA/n-BuOH (0.1/0.6/0.3) and (b) DBU/DMEA (0.2/0.0.57/0.23).

where m, σ, $y^{WCA}(\sigma)$ and A_{res}^{WCA} are the chain segment number, segment size, the cavity correlation function (Eq. (A3)) of monomer system and the residual Helmholtz free energy of the WCA system (Eq. (A4)) respectively.

$$y^{WCA}(\sigma) = 1 + \sum_{i=1}^{5}\sum_{j=1}^{5} b_{ij}\rho^{*i}T^{*(1-j)} \tag{A3}$$

$$\frac{A_{res}^{WCA}}{NkT} = -1.5lnT^{*} + \sum_{i=1}^{4}\sum_{j=1}^{4}\alpha_{ij}\rho^{*(1-i)}T^{*\frac{2-j}{2}} + \sum_{i=1}^{5} b_i\rho^{*i} + c_0 \tag{A4}$$

where $\rho^{*} = \rho\sigma^3$, $T^{*} = kT/\varepsilon$ and $c = (1 + 4\xi - 4\xi m^{-2})^{1/2}$ such that the parameter ξ is defined by Eq. (A5) and ρ is the chain number density.

$$\xi = \sum_{i=1}^{4}\sum_{j=1}^{4} c_{ij}\rho^{*i}T^{*(1-j)} \tag{A5}$$

where b_{ij} αij, bi, c_0 *and* c_{ij} are the coefficients of the above equations which are available in the published article by Mirzaeinia and Feyzi [29].

The RC term can be represented in the form of compressibility factor as follows:

$$Z^{RC} = \frac{\beta P}{\rho} = mZ^{WCA} - (m-1)\left(1 + \rho^* \frac{\partial \ln y^{WCA}(\sigma)}{\partial \rho^*}\right) + \rho^* \frac{d\ln\xi}{d\rho^*} \times \left[\frac{m}{2}\left(\frac{c}{1+4\xi} - 1\right) + \frac{2\xi}{1+4\xi}\right] \quad (A6)$$

where $\beta = 1/kT$ is the reciprocal temperature, P is the system pressure and Z^{WCA} is the compressibility factor for the fluid phase of WCA monomeric systems represented by Eq. (A7).

$$Z^{WCA}_{fluid} = 1 + \sum_{i=1}^{3}\sum_{j=1}^{4}(2i)\alpha_{ij}\rho^{*2i}T^{*(2-j)/2} + \sum_{i=1}^{5} i b_i \rho^{*i} \quad (A7)$$

The following mixing rules can be used to extend the RC contribution of the EoS to mixtures:

$$m = \sum_i x_i m_i \quad (A8)$$

$$\sigma^3_{mix} = \sum_i \sum_j x_i x_j \sigma^3_{ij} \quad (A9)$$

$$m^2 \varepsilon_{mix}\sigma^3_{mix} = \sum_i \sum_j x_i x_j m_i m_j \varepsilon_{ij}\sigma^3_{ij} \quad 10)$$

where x is the molar fraction and subscripts i and j indicate the property of components i and j in the mixture.

The combining rules are used to determine the cross parameters:

$$\sigma_{12} = \frac{\sigma_1 + \sigma_2}{2} \quad (A11)$$

$$\varepsilon_{12} = \sqrt{\varepsilon_1 \varepsilon_2}(1 - k_{12}) \quad (A12)$$

- *The dispersion term*:

The dispersion contribution is the sum of two separate terms of A_1 and A_2.

$$\frac{A^{disp}}{NkT} = \frac{A_1}{NkT} + \frac{A_2}{NkT} \quad (A13)$$

$$\frac{A_1}{NkT} = 2\pi\rho I_1(m,\eta)\sum_i\sum_j x_i x_j m_i m_j \left(\frac{\varepsilon_{ij}}{kT}\right)\sigma^3_{ij} \quad (A14)$$

$$\frac{A_2}{NkT} = -\pi\rho mkT\left(\frac{\partial\rho}{\partial P}\right)^{RC} I_2(m,\eta)\sum_i\sum_j x_i x_j m_i m_j \left(\frac{\varepsilon_{ij}}{kT}\right)^2 \sigma^3_{ij} \quad (A15)$$

where the integral equations of $I_1(m, \eta)$ and $I_2(m, \eta)$ are represented by:

$$I_1(m,\eta) = \sum_{i=1}^{5} a_i \eta^{i-1} \quad (A16)$$

$$I_2(m,\eta) = \sum_{i=1}^{5} a_i \eta^{i-1} \quad (A17)$$

$$a_i(m) = a_{i0} + a_{i1}\left(\frac{m-1}{m}\right) + a_{i2}\left(\frac{m-1}{m}\right)\left(\frac{m-2}{m}\right) \quad (A18)$$

The dispersion contribution in the form of compressibility factor is the sum of two separate terms of Z_1 and Z_2:

$$Z_1 = \frac{A_1}{NkT}\left(1 + \eta\frac{\partial \ln I_1(m,\eta)}{\partial\eta}\right) \quad (A19)$$

$$Z_2 = \frac{A_2}{NkT}\left(1 + \eta\frac{\partial \ln I_2(m,\eta)}{\partial\eta} + \eta\frac{\partial}{\partial\eta}\ln\left(Z^{RC} + \eta\frac{\partial Z^{RC}}{\partial\eta}\right)^{-1}\right) \quad (A20)$$

The LJ-Global TPT2 EoS has three pure component parameters: chain length m, segment diameter σ as the segment size parameter, and LJ potential depth ε as the dispersive interaction parameter.

- *The association term*:

$$\frac{A^{ass}_{res}}{NkT} = \sum_i x_i \sum_{A_i}\left[\ln X^{A_i} - \frac{1}{2}X^{A_i} + \frac{1}{2}\right] \quad (A21)$$

where X^{A_i} is the mole fraction of molecules i not bonded at site A:

$$X^{A_i} = \left(1 + \rho\sum_j x_j \sum_{B_j} X^{B_j}\Delta^{A_i B_j}\right)^{-1} \quad (A22)$$

$\Delta^{A_i B_j}$ is the association strength defined by Eq. (A23):

$$\Delta^{A_i B_j} = d^3_{ij} y^{WCA}(\sigma_{ij})\kappa^{A_i B_j}\left[\exp\left(\frac{\varepsilon^{A_i B_j}}{kT}\right) - 1\right] \quad (A23)$$

where $\varepsilon^{A_i B_j}$ and $\kappa^{A_i B_j}$ are the energy of association and the volume of association, respectively.

The compressibility factor is expressed as follow:

$$Z^{ass} = -\frac{\rho}{2}\sum_i x_i \sum_{A_i} X^{A_i}\sum_{A_i} x_j \sum_{B_j} X^{B_j}\Delta^{A_i B_j}\left(1 + \rho\left(\frac{\partial \ln g^{WCA}(\sigma_{ij})}{\partial\rho}\right)_{T,x_i}\right) \quad (A24)$$

Appendix B

The reactive bubble pressure calculation algorithm

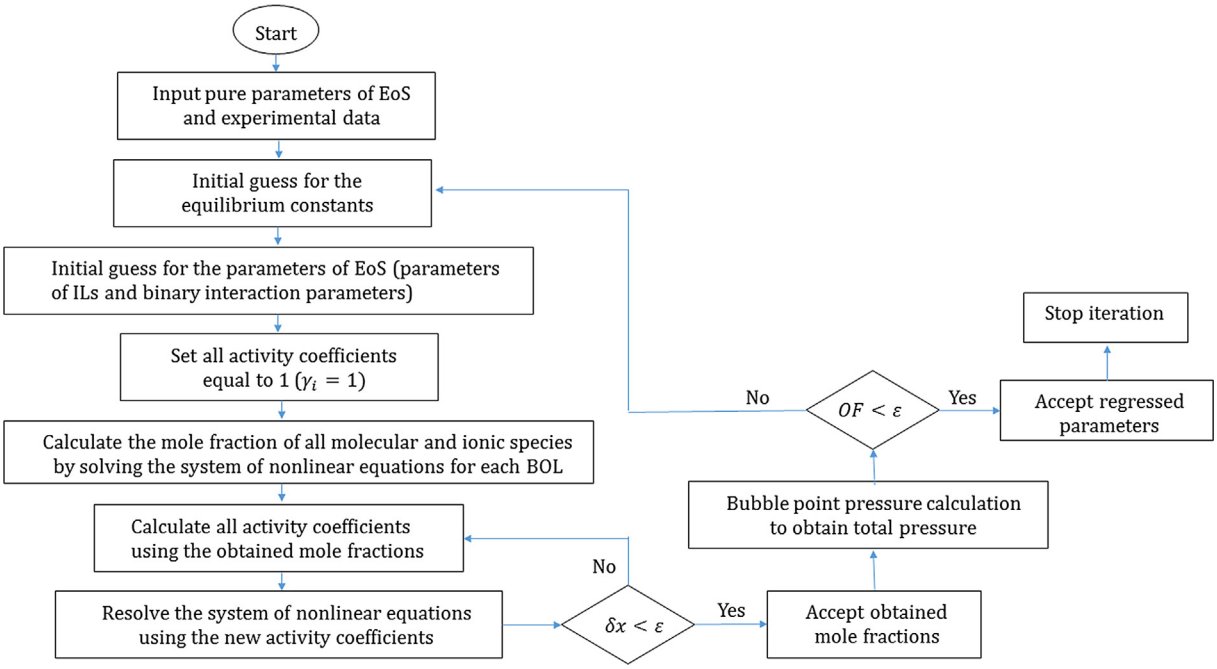

References

[1] T.U. Rashid, Ionic liquids: Innovative fluids for sustainable gas separation from industrial waste stream, J. Mol. Liq. 114916 (2020).
[2] G. Siani, M. Tiecco, P. Di Profio, S. Guernelli, A. Fontana, M. Ciulla, V. Canale, Physical absorption of CO_2 in betaine/carboxylic acid-based Natural Deep Eutectic Solvents, J. Mol. Liq. 315 (2020) 113708.
[3] M. Garip, N. Gizli, Ionic liquid containing amine-based silica aerogels for CO2 capture by fixed bed adsorption, J. Mol. Liq. 113227 (2020).
[4] A. Hafizi, M. Rajabzadeh, M.H. Mokari, R. Khalifeh, Synthesis, property analysis and absorption efficiency of newly prepared tricationic ionic liquids for CO_2 capture, J. Mol. Liq. 324 (2021) 115108.
[5] L.C. Barbosa, O.D.Q.F. Araújo, J.L. de Medeiros, Carbon capture and adjustment of water and hydrocarbon dew-points via absorption with ionic liquid [Bmim][NTf2] in offshore processing of CO_2-rich natural gas, J. Nat. Gas Sci. Eng. 66 (2019) 26–41.
[6] A. Hafizi, M.H. Mokari, R. Khalifeh, M. Farsi, M.R. Rahimpour, Improving the CO_2 solubility in aqueous mixture of MDEA and different polyamine promoters: The effects of primary and secondary functional groups, J. Mol. Liq. 297 (2020) 111803.
[7] F. Shakerian, K.H. Kim, J.E. Szulejko, J.W. Park, A comparative review between amines and ammonia as sorptive media for post-combustion CO_2 capture, Appl. Energy 148 (2015) 10–22.
[8] P.G. Jessop, D.J. Heldebrant, X. Li, C.A. Eckert, C.L. Liotta, Reversible nonpolar-to-polar solvent, Nature, 436(7054) (2005) 1102–1102.
[9] P.G. Jessop, S.M. Mercer, D.J. Heldebrant, CO_2-triggered switchable solvents, surfactants, and other materials, Energy Environ. Sci. 5 (6) (2012) 7240–7253.
[10] S. Kumar, J.H. Cho, I.L. Moon, Ionic liquid-amine blends and CO_2BOLs: Prospective solvents for natural gas sweetening and CO_2 capture technology—A review, Int. J. Greenhouse Gas Control 20 (2014) 87–116.
[11] E. Privalova, M. Nurmi, M.S. Marañón, E.V. Murzina, P. Mäki-Arvela, K. Eränen, J.P. Mikkola, CO_2 removal with 'switchable'versus 'classical'ionic liquids, Sep. Purif. Technol. 97 (2012) 42–50.
[12] C.J. Clarke, W.C. Tu, O. Levers, A. Brohl, J.P. Hallett, Green and sustainable solvents in chemical processes, Chem. Rev. 118 (2) (2018) 747–800.
[13] R. Hart, P. Pollet, D.J. Hahne, E. John, V. Llopis-Mestre, V. Blasucci, C.L. Liotta, Benign coupling of reactions and separations with reversible ionic liquids, Tetrahedron 66 (5) (2010) 1082–1090.
[14] P.M. Mathias, F. Zheng, D.J. Heldebrant, A. Zwoster, G. Whyatt, C.M. Freeman, P. Koech, Measuring the Absorption Rate of CO2 in Nonaqueous CO_2-Binding Organic Liquid Solvents with a Wetted-Wall Apparatus, ChemSusChem 8 (21) (2015) 3617–3625.
[15] D.J. Heldebrant, C.R. Yonker, P.G. Jessop, L. Phan, Organic liquid CO_2 capture agents with high gravimetric CO_2 capacity, Energy Environ. Sci. 1 (4) (2008) 487–493.
[16] T. Yamada, P.J. Lukac, T. Yu, R.G. Weiss, Reversible, room-temperature, chiral ionic liquids. Amidinium carbamates derived from amidines and amino-acid esters with carbon dioxide, Chem. Mater. 19 (19) (2007) 4761–4768.
[17] T. Yu, T. Yamada, G.C. Gaviola, R.G. Weiss, Carbon dioxide and molecular nitrogen as switches between ionic and uncharged room-temperature liquids comprised of amidines and chiral amino alcohols, Chem. Mater. 20 (16) (2008) 5337–5344.
[18] T. Yamada, P.J. Lukac, M. George, R.G. Weiss, Reversible, room-temperature ionic liquids. Amidinium carbamates derived from amidines and aliphatic primary amines with carbon dioxide, Chem. Mater. 19 (5) (2007) 967–969.
[19] D.J. Heldebrant, P.K. Koech, J.E. Rainbolt, F. Zheng, T. Smurthwaite, C.J. Freeman, I. Leito, Performance of single-component CO2-binding organic liquids (CO_2BOLs) for post combustion CO_2 capture, Chem. Eng. J. 171 (3) (2011) 794–800.
[20] V.M. Blasucci, R. Hart, P. Pollet, C.L. Liotta, C.A. Eckert, Reversible ionic liquids designed for facile separations, Fluid Phase Equilib. 294 (1–2) (2010) 1–6.
[21] F. Liu, G. Jing, B. Lv, Z. Zhou, High regeneration efficiency and low viscosity of CO_2 capture in a switchable ionic liquid activated by 2-amino-2-methyl-1-propanol, Int. J. Greenhouse Gas Control 60 (2017) 162–171.
[22] O.Y. Orhan, E. Alper, Kinetics of carbon dioxide binding by promoted organic liquids, Chem. Eng. Technol. 38 (8) (2015) 1485–1489.
[23] A. Hedayati, F. Feyzi, CO_2-binding organic liquids comprised of 1, 1, 3, 3-Tetramethylguanidine and alkanol for post combustion CO_2 capture: water inhibitory effect of amine promoters, ACS Sustainable Chem. Eng. (2020).
[24] A. Hedayati, F. Feyzi, Towards water-insensitive CO_2-binding organic liquids for CO2 absorption: Effect of amines as promoter, J. Mol. Liq. 112938 (2020).
[25] J.E. Rainbolt, P.K. Koech, C.R. Yonker, F. Zheng, D. Main, M.L. Weaver, D.J. Heldebrant, Anhydrous tertiary alkanolamines as hybrid chemical and physical CO_2 capture reagents with pressure-swing regeneration, Energy Environ. Sci. 4 (2) (2011) 480–484.
[26] A. Mirzaeinia, F. Feyzi, A perturbed-chain equation of state based on Wertheim TPT for the fully flexible LJ chains in the fluid and solid phases, J. Chem. Phys. 152 (13) (2020) 134502.
[27] A. Mirzaeinia, F. Feyzi, S.M. Hashemianzadeh, Equations of state for the fully flexible WCA chains in the fluid and solid phases based on Wertheims-TPT2, J. Chem. Phys. 148 (10) (2018) 104502.
[28] A. Mirzaeinia, F. Feyzi, S.M. Hashemianzadeh, Equation of state and Helmholtz free energy for the atomic system of the repulsive Lennard-Jones particles, J. Chem. Phys. 147 (21) (2017) 214503.

[29] M. Wagner, I. von Harbou, J. Kim, I. Ermatchkova, G. Maurer, H. Hasse, Solubility of carbon dioxide in aqueous solutions of monoethanolamine in the low and high gas loading regions, J. Chem. Eng. Data 58 (4) (2013) 883–895.
[30] D.Y. Peng, D.B. Robinson, A new two-constant equation of state, Ind. Eng. Chem. Fundam. 15 (1) (1976) 59–64.
[31] D.P. Shoemaker, C.W. Garland, J.I. Steinfeld, Experiments in physical chemistry, McGraw-Hill, 2018.
[32] S. García-Argüelles, M.L. Ferrer, M. Iglesias, F. Del Monte, M.C. Gutiérrez, Study of Superbase-Based Deep Eutectic Solvents as the Catalyst in the Chemical Fixation of CO_2 into Cyclic Carbonates under Mild Conditions, Materials 10 (7) (2017) 759.
[33] L. Phan, D. Chiu, D.J. Heldebrant, H. Huttenhower, E. John, X. Li, P.G. Jessop, Switchable solvents consisting of amidine/alcohol or guanidine/alcohol mixtures, Ind. Eng. Chem. Res. 47 (3) (2008) 539–545.
[34] A. Hedayati, S.M. Ghoreishi, Supercritical carbon dioxide extraction of glycyrrhizic acid from licorice plant root using binary entrainer: experimental optimization via response surface methodology, The Journal of Supercritical Fluids 100 (2015) 209–217.
[35] A. Najafloo, A.T. Zoghi, F. Feyzi, Measuring solubility of carbon dioxide in aqueous blends of N-methyldiethanolamine and 2-((2-aminoethyl) amino) ethanol at low CO_2 loadings and modelling by electrolyte SAFT-HR EoS, J. Chem. Thermodyn. 82 (2015) 143–155.
[36] K.M. De Reuck, V.V. Altunin, O.G. Gadetskii, G.A. Chapela, J.S. Rowlinson, in: Carbon dioxide, Pergamon Press, Oxford, 1976, p. (p. 385)..
[37] A. Ostonen, E. Sapei, P. Uusi-Kyyny, A. Klemelä, V. Alopaeus, Measurements and modeling of CO_2 solubility in 1, 8-diazabicyclo-[5.4. 0]-undec-7-ene-Glycerol solutions, Fluid Phase Equilib. 374 (2014) 25–36.
[38] S. Lin, H. Lu, Y. Liu, C. Liu, B. Liang, K. Wu, Density studies of 1, 8-diazabicyclo [5.4. 0] undec-7-ene (DBU)-glycerol and CO_2-DBU-glycerol solutions at temperatures between 288.15 K and 328.15 K, J. Chem. Thermodyn. 123 (2018) 8–16.
[39] D. Lipkind, N. Rath, J.S. Chickos, V.A. Pozdeev, S.P. Verevkin, The Vaporization Enthalpies of 2-and 4-(N, N-Dimethylamino) pyridine, 1, 5-Diazabicyclo [4.3. 0] non-5-ene, 1, 8-Diazabicyclo [5.4. 0] undec-7-ene, Imidazo [1, 2-a] pyridine and 1, 2, 4-Triazolo [1, 5-a] pyrimidine by Correlation–Gas Chromatography, J. Phys. Chem. B, 115(27) (2011) 8785–8796.
[40] A. Ostonen, P. Uusi-Kyyny, M. Pakkanen, V. Alopaeus, Dew points of pure DBN and DBU and vapor–liquid equilibria of water+ DBN and water+ DBU systems for cellulose solvent recycling, Fluid Phase Equilib. 408 (2016) 79–87.
[41] P. Stephan, S. Kabelac, M. Kind, D. Mewes, K. Schaber, T. Wetzel, (Eds.). (2019). VDI heat atlas: Professional sponsor of the VDI Society for Process Engineering and Chemical Engineering, Springer publishing house.
[42] T.E. Daubert, R.P. Danner, H.M. Sibul, C.C. Stebbins, Physical and Thermodynamic Properties of Pure Chemicals: Data Compilation, Taylor & Francis, Washington, DC, 1989.
[43] D.D. Pinto, J.G.S. Monteiro, B. Johnsen, H.F. Svendsen, H. Knuutila, Density measurements and modelling of loaded and unloaded aqueous solutions of MDEA (N-methyldiethanolamine), DMEA (N, N-dimethylethanolamine), DEEA (diethylethanolamine) and MAPA (N-methyl-1, 3-diaminopropane), Int. J. Greenhouse Gas Control 25 (2014) 173–185.
[44] K. Klepácová, P.J. Huttenhuis, P.W. Derks, G.F. Versteeg, Vapor pressures of several commercially used alkanolamines, J. Chem. Eng. Data 56 (5) (2011) 2242–2248.
[45] N. Chiali-Baba-Ahmed, F. Dergal, L. Negadi, I. Mokbel, Measurement and correlation of the (vapor+ liquid) equilibria of pure 4-ethylmorpholine, 1, 2-dimethylisopropylamine and N, N-dimethylethanolamine, and their binary aqueous solutions, J. Chem. Thermodyn. 63 (2013) 44–51.
[46] C. Secuianu, V. Feroiu, D. Geana, High-pressure vapor– liquid equilibria in the system carbon dioxide and 2-propanol at temperatures from 293.25 K to 323.15 K, J. Chem. Eng. Data, 48(6) (2003) 1384-1386.
[47] H.I. Chen, H.Y. Chang, P.H. Chen, High-pressure phase equilibria of carbon dioxide+ 1-butanol, and carbon dioxide+ water+ 1-butanol systems, J. Chem. Eng. Data 47 (4) (2002) 776–780.
[48] G. Silva-Oliver, L.A. Galicia-Luna, Vapor–liquid equilibria near critical point and critical points for the CO_2+1-butanol and CO_2+2-butanol systems at temperatures from 324 to 432 K, Fluid Phase Equilib. 182 (1–2) (2001) 145–156.